

Original paper

Geochemistry and petrology of high-pressure kyanite–garnet–albite–K-feldspar felsic gneisses and granulites from the Kutná Hora Complex, Bohemian Massif

Stanislav VRÁNA*, Veronika ŠTĚDRÁ, Radmila NAHODILOVÁ

Czech Geological Survey, Klárov 3, 118 21 Prague 1, Czech Republic; stanislav.vrana@geology.cz

* Corresponding author



The Kutná Hora Complex (KHC), bordering the Moldanubian Zone at the north, represents a crustal stack of several allochthonous units. This study presents new interpretation based on detailed whole-rock geochemical analyses, petrology, mineral analyses and geothermobarometric calculations. Samples were selected from the Malín and the Běstvina units, with preference for kyanite-bearing albitic felsic gneisses with high-pressure metamorphic record.

Three types of kyanite-garnet-albite-K-feldspar rocks studied include: (1) an early Variscan felsic granulite from the Běstvina Unit equilibrated under eclogite-facies conditions ($P = 1.8\text{--}2.1$ GPa, metamorphic event M_1), (2) a garnet-kyanite leucosome from a polymetamorphic migmatite ($P \sim 1.6$ GPa, metamorphic event M_2), and (3) a felsic kyanite-garnet-muscovite gneiss derived from garnetiferous leucogranite, equilibrated under amphibolite-facies conditions ($P = 0.9\text{--}1.1$ GPa, metamorphic event M_3). All the three rock types exhibit geochemical characteristics of highly evolved leucogranitic rocks with low Zr/Hf ratios (14 to 19), relatively low FeOt/MnO (10 to 33), and contain < 30 ppm Zr, < 15 ppm Y, and low ΣREE (< 28 ppm) abundances. The kyanite-garnet-muscovite felsic gneiss contains locally garnet porphyroclasts up to 3 cm in diameter, with up to 28 mol. % spessartine and 0.55 wt. % P_2O_5 , which represent relics from the magmatic stage of the garnetiferous leucogranite precursor. Accessory tourmaline (dravite-schorl) and dumortierite occur in migmatitic gneisses of the Malín Unit, while dumortierite is common in the felsic gneiss (M_3). Textural relationships indicate a late, post-kinematic growth of tourmaline and dumortierite in relation to D_3/M_3 .

The repetitive high-pressure record manifested during three metamorphic events in the Kutná Hora Complex represents a unique example in the Bohemian Massif. These relations indicate a separate evolution of the Kutná Hora Complex and the Moldanubian Zone during much of their Variscan tectonometamorphic history. Several aspects of possible correlation among the Kutná Hora Complex (plus the Svatka Unit) and the Orlice-Sněžník Unit at the Czech-Polish border, which all have a record of Palaeo-Variscan (U)HP evolution, are discussed.

Keywords: felsic gneiss, felsic granulite, leucogranite precursors, high-pressure metamorphism, polymetamorphism, Kutná Hora Complex

Received: 12 March 2009; accepted: 12 June 2009; handling editor: J. Kotková

The online version of this article (<http://dx.doi.org/10.3190/jgeosci.045>) contains supplementary electronic material.

1. Introduction

O'Brien and Rötzler (2003, tab. 1) and Janoušek et al. (2006a, tab. 8) pointed out the strong contrasts in PTt histories among the individual Variscan granulite bodies of the Bohemian Massif. Geochemical evidence shows that the most widespread felsic kyanite-garnet granulites of leucogranite-granite composition were dominantly derived from Lower Palaeozoic calc-alkali magmatic rocks (Janoušek et al. 2004). Nonetheless, other compositional types of granulites, such as highly differentiated rocks, are also of interest since they carry information, which is not revealed by studying the most widespread calc-alkali granulite types (Vrána 1989; Janoušek et al. 2006a, 2007; Kotková 2007; this study).

The Kutná Hora Complex (KHC), situated between the internal high-grade Variscan Moldanubian Zone and the

structurally overlying low-grade (mainly Neoproterozoic) Bohemian Zone, contains some of these interesting granulite and felsic gneiss types. The aim of our study is to constrain the metamorphic history of the KHC, focusing especially on its contrasting features in comparison with metamorphic patterns characteristic of the neighbouring parts of the Moldanubian Zone as qualitatively indicated by data presented for KHC by Synek and Oliveriová (1993), Owen and Dostal (1996) and Tajčmanová et al. (2006) for the NE part of the Moldanubian Zone. The main methods of study were detailed whole-rock geochemical characteristics including trace elements, together with petrology and mineral chemistry used for geothermobarometric interpretation.

The studied samples include kyanite-garnet-muscovite-albite-K-feldspar felsic gneisses from the Malín Unit (Figs 1–2). A kyanite-garnet-albite-K-feldspar

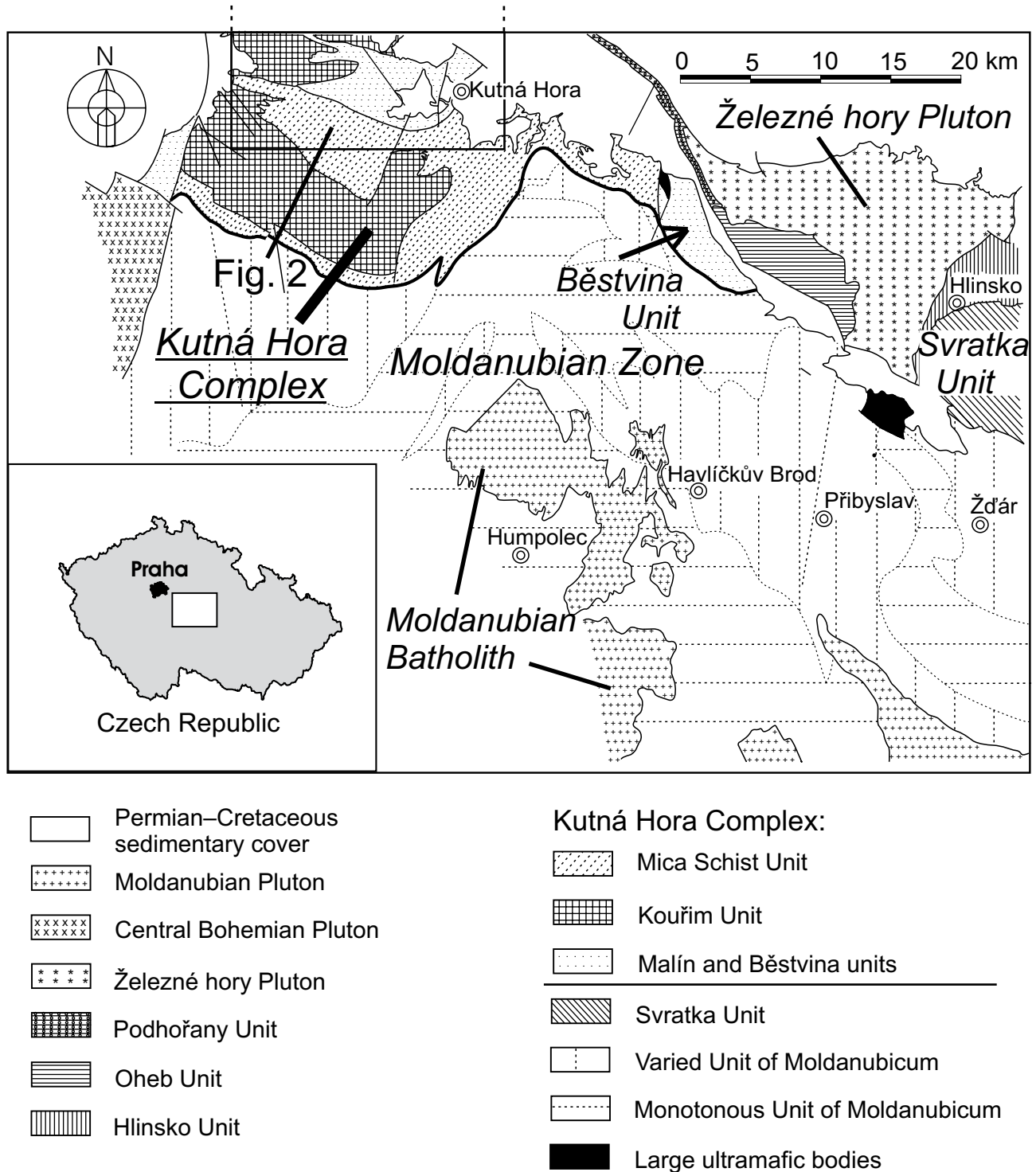


Fig. 1 Geological setting of the studied area in the Kutná Hora Complex, modified after Synek and Oliveriová (1993).

leucosome from polymetamorphic migmatite in the same unit is also included for comparison. The Běstvína Unit is dominated by felsic granulites of calc-alkali leucogranite and granite composition, but samples 5 and 6 from the set studied by Vrána et al. (2005) are albite–K-feldspar felsic granulites equilibrated under eclogite-facies conditions.

The felsic gneisses from the Malín Unit and the albite granulite from the Běstvína Unit are compared with calc-alkali kyanite–garnet granulites of granitic composition and biotite–kyanite–garnet granulite (of Fe-rich paragneiss composition) from the Běstvína Unit. The aim is to show the differences in the whole-rock geochemistry

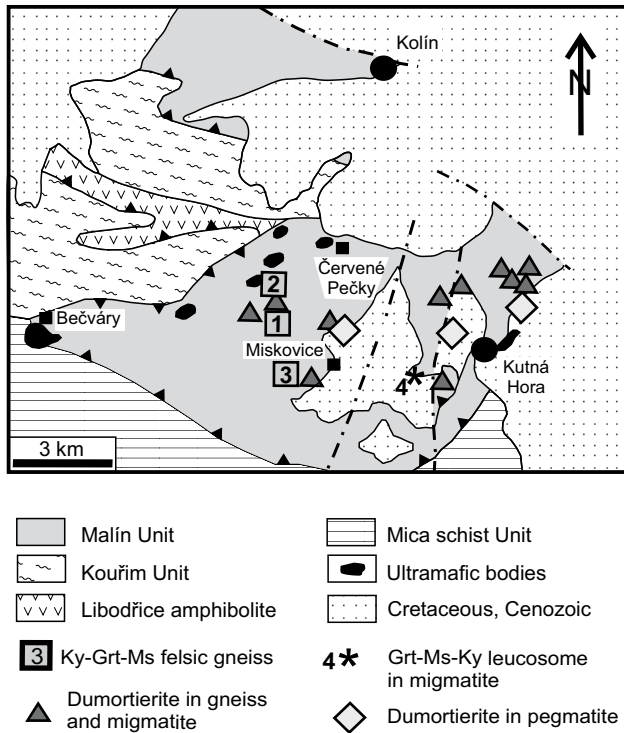


Fig. 2 Location of the studied samples (Nos 1 to 4) and dumortierite localities near Kutná Hora. Dumortierite localities after Losert (1956a), geology modified after Synek and Oliveriová (1993). Symbols for the individual samples overlap the location of villages and other places mentioned in text as local names (Tab. 1). Please refer to the online map at <http://dx.doi.org/10.3190/jgeosci.045>.

(protolith composition) and in the metamorphic record among samples from the Kutná Hora Complex.

Attention is paid to accessory tourmaline and dumortierite, present both in the felsic gneisses and in the polymetamorphic leucosome. This information will be important for understanding the timing and conditions of emplacement of the dumortierite pegmatites (Cempírek and Novák 2006) in the KHC in relation to the general sequence of events in this unit.

When dealing with metamorphosed igneous rocks, it is often useful to refer to the terminology of the corresponding magmatic rocks. The reason for accurate discrimination of the various felsic rock types are the occurrences of garnetiferous hyperpotassic syenitic alkali-feldspar granulites and alkali-feldspar (granitic) granulites in southern Bohemia (Vrána 1989), and the fact that this study deals with some geochemically highly evolved rock types.

According to the IUGS classification of igneous rocks (Le Maitre 1989), a compositional limit of $An < 5$ mol. % is set for inclusion of albitic plagioclase among alkali feldspars. This limiting value is significant in terminology, e.g. *alkali-feldspar granite* vs. *granite* ("normal", calc-alkali granite). Because many of the samples studied

have plagioclase composition in the range of An_2 to An_9 , we use the designation albite–K-feldspar granulite (or precursor granite), to avoid confusion.

2. Geological setting

The Kutná Hora Complex (KHC) is situated between the internal Variscan Moldanubian Zone and the structurally overlying low-grade (mainly Neoproterozoic) Bohemian Zone (Fig. 1). The introductory information on regional geology and structure of the wider area is presented in the accompanying paper by Verner et al. (this volume). The uppermost part of the KHC is divided into three units:

- 1) **Běstvina Unit** (Losert 1967), built by felsic granulites and partly migmatized gneisses with lenses of garnet peridotites, eclogites, and rare garnet amphibolites; the unit which is 8 by 3 km in size, constitutes the southeastern segment of the Kutná Hora Complex (Fig. 1),
- 2) **Malín Unit** (Malín Formation of Losert 1956a, b) consisting mainly of leucocratic kyanite-bearing migmatites accompanied by garnet amphibolites, partly serpentinized garnet peridotites, eclogites and several skarn bodies,
- 3) **Plaňany Unit** (Fišera 1977) built by various types of migmatites (metasedimentary and metaigneous mafic) with lenses of amphibolites, serpentinites and pyroxenites; no samples from this unit were included in the present study; the small unit is located NW of the area shown in Fig. 2,
- 4) the underlying units represented by the **Kouřim Unit** consisting of orthogneiss with fine-grained leucocratic migmatites and by the lowermost **Mica Schist Unit** consisting of metapelites intercalated with amphibolites (Synek and Oliveriová 1993) (Fig. 2).

According to Synek and Oliveriová (1993), rocks of the Malín Unit were involved in several deformation (D)/metamorphism (M) events: the D_1/M_1 event coincided with crystallization and emplacement of garnet peridotites/lherzolites (dated at 377 ± 20 Ma, Brueckner et al. 1991), eclogitization of basic rocks and metamorphic crystallization of HP/HT granulites. The S_1 metamorphic foliation is generally subvertical or steeply dipping to the NE, but rarely preserved in the Běstvina and Malín units (Nahodilová et al. 2005). The D_2/M_2 event is characterized as a mylonitization and retrogression event in HP eclogite/amphibolite-facies, reworking the older S_1 fabrics into a flat penetrative S_2 foliation dipping to the NW or NE. Accompanied was by a late-stage partial melting and migmatization generating kyanite-bearing leucosomes. The D_3/M_3 event produced S_3 mylonitic axial cleavage and foliation with newly crystallized biotite and muscovite (\pm garnet, kyanite) under HP amphibolite-facies conditions.

Following the interpretation by Synek and Oliveriová (1993), the units comprising the Kutná Hora Complex represent a stack of allochthonous segments of crustal rocks with lenses of upper-mantle pyrope peridotite/lherzolite up to 1 km long. The thrusting probably took place before the D_3 event. Data on crustal eclogite and garnet peridotites in the Běstvina Unit were presented by Medaris et al. (2006) and Faryad (2009).

3. Methodology

3.1. Samples

The studied lithologies include three rock types representing parts of the Malín Unit and the Běstvina Unit. The criterion for sample selection was the modal presence of garnet, kyanite and albitic plagioclase. The samples were selected from a large sample set studied in connection with geological mapping of the Kutná Hora area on the scale of 1:25 000 by one of the authors (Štědrá et al. 2009). In addition, we used several granulite samples from the Běstvina Unit characterised by Vrána et al. (2005).

The kyanite–garnet–muscovite felsic gneiss, exposed in abandoned quarries south of Bohouňovice (sometimes referred to as the Bořetice locality – Fiala et al. 1982; Fiala 1992) and northeast of the village of Suchdol (Fig. 2), occurs as compositionally homogeneous layers up to 25 m thick. It is represented by samples 2 and 501 taken from the same outcrop. Sample 501 is identical with sample 2, except for the presence of widely scattered, large garnet porphyroclasts in the former sample.

The bodies extend along the strike of the country rock for a distance of several hundred metres, resembling an aplite sheet (Fiala 1992). The country rocks are represented by the migmatitic kyanite–garnet–muscovite paragneiss and the muscovite–biotite paragneiss of the Malín Unit (Synek and Oliveriová 1993). Fiala (1992) noted the presence of thin (several cm thick) sills and discordant dykes in the proximity of the main felsic gneiss body. Fiala et al. (1982) and Fiala (1992) wrote that the “felsic gneisses are of granulitic character (approx. $T = 700\text{ °C}$, $P = 0.9\text{ GPa}$), their genesis cannot be separated from gneissic surroundings, and it is therefore reasonable to suppose the HP granulite metamorphism for the Malín Unit (‘Malín Formation’) as a whole”.

A garnet–muscovite–kyanite leucosome from the polymetamorphic migmatite in the Bylanka brook at outskirts of Kutná Hora (sample 4) was studied as an example of the Malín Unit migmatites.

The studied garnet–kyanite–albite–K-feldspar granulite (samples 5 and 6) from the Běstvina Unit is exposed on a 20 m high cliff in the Doubrava River valley *c.* 400 m

west of the village of Spačice (Faryad 2009). Garnet–kyanite granulites predominantly of calc-alkali granite (leucogranite) composition, (Fiala et al. 1987; Vrána et al. 2005), represent the main rock type of the Běstvina Unit (samples 7 and 8).

Although geochemical data for the Běstvina granulite samples were presented recently (Vrána et al. 2005), minor- and trace-element abundances were newly analyzed by more accurate methods, performed in the same laboratory as the trace-element analyses for the recently studied Ab–Kfs rocks from the KHC. For comparison, new data from several granulite samples from the Běstvina Unit are included here.

Fiala et al. (1982) published a comparative mineralogical and major-element whole-rock geochemical study of kyanite-bearing felsic gneisses from the KHC, accompanied by several samples of granulites from the Běstvina Unit and from the Moldanubian Zone, all designated as “leptynites”. The trace-element concentrations in the samples were not determined. Later on, Fiala et al. (1987) published several analyses of felsic granulites from the Běstvina Unit.

3.2. Analytical methods

Major-element whole-rock analyses were performed by wet chemical methods in the laboratory of the Czech Geological Survey, Prague. Minor and trace elements were analysed in the Acme Analytical Laboratories, Vancouver, Canada, using $\text{LiBO}_2/\text{Li}_2\text{B}_4\text{O}_7$ fusion and ICP–MS/ES. Precious and base metals were determined by aqua regia digestion and ICP–MS.

Mineral analyses were carried out using the CAMECA SX 100 WDS electron microprobe at the Joint Laboratory of Electron Microscopy and Microanalysis, Institute of Geological Sciences, Masaryk University and Czech Geological Survey, Brno. The analytical conditions were adjusted to the type of mineral analysed, usually 15 kV accelerating voltage, probe current 10–20 nA, acquisition time 10–30 s. The standards used were spessartine (Si, Mn), almandine (Fe), andradite (Ca), MgAl_2O_4 (Mg), hornblende (Ti), sanidine (Al, K), albite (Na), fluorapatite (P) and chromite (Cr). Mineral abbreviations in this paper are those of Kretz (1983).

4. Petrography

4.1. Fine-grained felsic gneisses

Mineralogical and selected whole-rock geochemical indices for the studied rocks are given in Tab. 1. The felsic rocks are very fine-grained, with garnet typically smaller than 2 mm. Foliation planes are incompletely covered by

Tab. 1 Mineralogy, oxide and element ratios in felsic gneisses and granulites

| Sample No. | Locality | WGS-84-N | WGS-84-E | Grt | Ms | Ky | Du | An _M | An _N | ASI | FeO [†] | FeO [†] /MgO | FeO [†] /MnO | Zr/Hf | Total REE | La _N /Yb _N | Eu/Eu* |
|------------------|--------------------|-------------|-------------|-----|----|----|----|-----------------|-----------------|------|------------------|-----------------------|-----------------------|-------|-----------|----------------------------------|--------|
| 1 | Suchdol | 49°57'19.2" | 15°10'37.2" | + | + | + | + | 5 | 4 | 1.14 | 1.01 | 12.63 | 13.8 | 13.93 | 10.50 | 1.78 | 0.816 |
| 2 | Bohouňovice quarry | 49°58'7.4" | 15°10'42.2" | + | + | + | + | 6 | 7 | 1.26 | 0.90 | 15.00 | 15.8 | 15.71 | 13.61 | 2.22 | 0.783 |
| 501 [†] | Bohouňovice quarry | 49°58'7.4" | 15°10'42.2" | + | + | + | + | | | | | | | | | | |
| 3 | Bohouňovice-Vysoká | 49°56'29.9" | 15°11'23.9" | tr | + | | + | 5 | 4 | 1.10 | 0.39 | 3.25 | 32.5 | 18.83 | 27.63 | 3.57 | 1.911 |
| 4 | Kutná Hora-Bylanka | 49°56'30.8" | 15°14'52.7" | + | + | + | + | 4 | 2 | 1.18 | 0.78 | 11.14 | 10.3 | 19.00 | 7.99 | 2.80 | 0.430 |
| 5 | Běstvína-Spačice | 49°49'7.3" | 15°35'26.7" | + | | + | | 8 | 9 | 1.37 | 1.75 | 1.22 | 30.2 | 18.67 | 73.14 | 5.47 | 0.574 |
| 6 | Běstvína-Spačice | 49°49'7.3" | 15°35'26.7" | + | | + | | | | | | | | 22.67 | 24.96 | 4.77 | 0.634 |
| 7 | Běstvína-Spačice | 49°49'2.7" | 15°35'15.1" | + | tr | + | | 18 | 19 | 1.12 | 2.39 | 4.35 | 50.9 | | 103.55 | 4.50 | 0.470 |
| 8 | Běstvína-Pařížov | 49°49'44.6" | 15°34'14.6" | + | | + | | 15 | 17 | 1.23 | 2.39 | 4.35 | 45.1 | 27.10 | 105.02 | 4.08 | 0.346 |
| 9 | Běstvína-Spačice | 49°49'17.8" | 15°35'50.7" | + | | + | | 15 | 29 | 2.13 | 7.82 | 2.70 | 81.5 | 30.13 | 224.74 | 7.15 | 0.698 |

Note:

An_M – plagioclase composition measured, An_N – normative plagioclase composition (CIPW), ASI – alumina saturation index, tr – traces

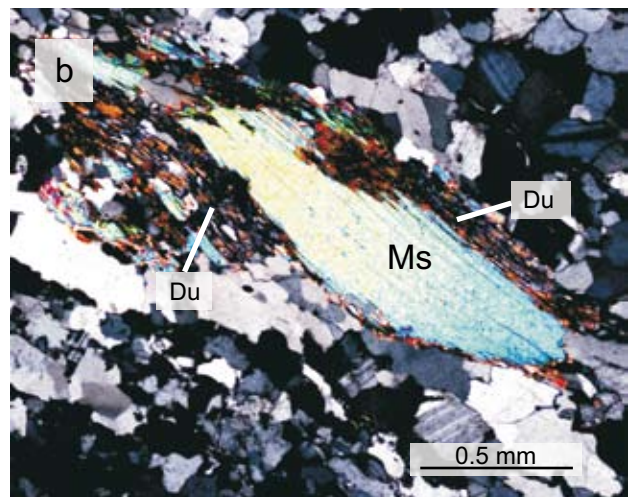
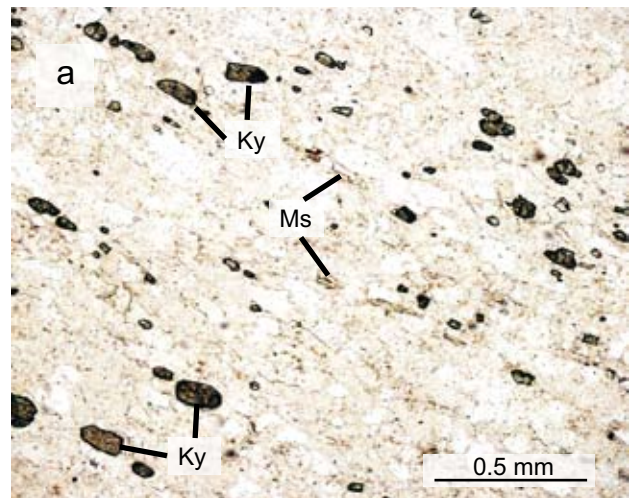
† – sample 501 was used for microprobe analyses of minerals and study of large relict Grt porphyroclasts

Rock types: 1–3 – Grt-Ky-Ms felsic gneiss; 4 – Grt-Bt-Ms-Ky leucosome; 5–6 – Grt-Ky felsic granulite (albitic); 7–8 – Grt-Ky felsic granulite (Běstvína Unit); 9 – Bt-Ky-Grt granulitic gneiss (metasedimentary)

muscovite. Quartz is commonly separated into mono-mineralic ribbons less than 1 mm thick, which alternate with feldspathic bands of albite and weakly perthitic fine-grained (0.1 to 0.5 mm long) K-feldspar. The latter bands contain kyanite (up to ~3 vol. %) and/or muscovite (Fig. 3a). Lenticular porphyroclasts of 1 mm long K-feldspar and large primary (?) muscovite I are deformed to fish-like shapes (Fig. 3b). There are local aggregates, up to several dm² in size, with coarse garnet (6 to 30 mm in diameter) intergrown with quartz. An additional sample 501 from the same outcrop as the sample 2 was used for characterization of the large garnet porphyroclasts and matrix minerals. In the matrix, garnet is present as anhedral crystals less than 1 mm in diameter. The modal contents of muscovite II and kyanite show variations (muscovite content from minor to *c.* 5 vol. %) across the foliation. Kyanite has not been observed as inclusions in garnet. Minor dumortierite forms violet fibrous aggregates in the felsic matrix; light blue dumortierite is rare. Apatite and subordinate graphite are accessories; apatite is pale yellow in thin sections and occurs locally as small porphyroclasts but exceptionally a single 1 cm long apatite crystal has been observed. Accessory tourmaline and rutile, reported by Fiala et al. (1982) and Fiala (1992), were not found.

⇒

Fig. 3 a – Kyanite and muscovite in Qtz–Ab–Kfs mylonitic matrix of felsic gneiss, sample 2, Bohouňovice; garnet is present in other parts of thin section; plain polarized light; **b** – Deformed porphyroclast of primary muscovite I rimmed by dumortierite (Du) in mylonitic matrix of felsic gneiss, sample 2, Bohouňovice; crossed polarizers.



Sample 3 from the Vysoká Hill (Fig. 2) is somewhat different from samples 1 and 2 in that it contains only traces of garnet confined to local biotite-rich laminae. Garnet in this sample was probably extensively consumed by the reaction $\text{Grt} + \text{Kfs} + \text{H}_2\text{O} \rightarrow \text{Bt}$. Biotite aggregates are seen on foliation planes as patches 5×30 mm in size and less than 1 mm thick. The total biotite content in the rock is estimated to less than 3 vol. %. In addition to biotite aggregates, foliation planes are partly covered by muscovite. Kyanite is absent in this sample, which may be a result of its replacement by muscovite. On a microscopic scale, there are two types of a late tourmaline: khaki-coloured anhedral grains nucleated at places with Ti available from biotite, followed by a low-Ti tourmaline of light bluish-green colour. The late, light bluish-green tourmaline is subhedral to euhedral, somewhat skeletal due to quartz inclusions, and rimmed by a narrow zone of quartz. Fibrous aggregates of violet dumortierite are present in the felsic matrix. The aggregates are oriented both parallel and across the mylonitic foliation, indicating, together with the skeletal and subhedral crystals of the bluish-green tourmaline, late post-mylonitic (post- D_3) crystallization of the borosilicates. Dumortierite and tourmaline are minor accessories, which occur in different domains of the samples and exhibit no reaction relationship.

4.2. Foliated leucosome from polymetamorphic migmatite

Sample 4 (Tab. 1) from the left tributary of the Bylanka brook in the outskirts of the city of Kutná Hora is another example of Ab-Kfs garnet-kyanite-muscovite felsic rock in the KHC. The sample is dominated by pale pink feldspars and shows a mylonitic foliation. The foliation is defined by several mm long lenticular quartz aggregates grading to quartz ribbons, oriented flakes of early deformed muscovite I, 1–7 mm long, and 1×3 cm aggregates of bluish kyanite, with individual crystals up to 3 mm in size. Garnet, relatively coarse kyanite and albite are pre-mylonitization phases, which can be used for pressure estimation of the early HP/HT M_2 event. Biotite aggregates, marginally replacing garnet (5 mm in diameter), or locally replacing older coarse muscovite I, can be observed. The foliation planes are partly covered by small, newly formed muscovite II. Rare xenoblastic khaki-coloured tourmaline up to 1 mm in diameter occurs intergrown with biotite in the proximity of garnet. Skeletal bluish-green tourmaline, similar to the tourmaline in the sample 3, occurs locally along the boundary between the quartz ribbon and a feldspathic band. The rock contains numerous fibrous aggregates (1 mm in diameter) of randomly oriented violet dumortierite. Dumortierite

Tab. 2 Major-element whole-rock chemical analyses for felsic gneisses and granulites (wt. %)

| Sample No. | 1 | 2 | 3 | 4 | 5 | 7 | 8 | 9 |
|---|-----------------|---------------------|----------|----------|---------|---------|--------------|----------------|
| No. | KK30G | KMV43 | KH47 | KH126 | MF153 | KK72S | KMV98 | MF7 |
| Locality | Suchdol, quarry | Bohouňovice, quarry | Vysoká | Bylanka | Spačice | Spačice | Pařížov, dam | Spačice, north |
| SiO ₂ | 74.64 | 74.03 | 73.84 | 76.92 | 76.40 | 77.67 | 73.26 | 59.18 |
| TiO ₂ | 0.03 | 0.01 | 0.07 | 0.04 | 0.14 | 0.09 | 0.10 | 0.50 |
| Al ₂ O ₃ | 14.41 | 14.97 | 14.46 | 12.85 | 12.91 | 10.78 | 13.96 | 19.58 |
| Fe ₂ O ₃ | 0.22 | 0.16 | – | – | 0.35 | 0.23 | 0.26 | 1.11 |
| FeO | 0.81 | 0.76 | – | – | 1.43 | 2.18 | 2.16 | 6.82 |
| Fe ₂ O ₃ ¹ | – | – | 0.43 | 0.87 | – | – | – | – |
| MnO | 0.073 | 0.057 | 0.012 | 0.076 | 0.058 | 0.047 | 0.053 | 0.096 |
| MgO | 0.08 | 0.06 | 0.12 | 0.07 | 1.43 | 0.55 | 0.55 | 2.90 |
| CaO | 0.62 | 0.77 | 0.70 | 0.48 | 0.86 | 1.08 | 1.13 | 1.62 |
| Li ₂ O | – | – | 0.002 | 0.002 | 0.023 | – | 0.007 | 0.011 |
| Na ₂ O | 4.59 | 4.18 | 4.45 | 3.86 | 3.21 | 1.89 | 2.76 | 2.12 |
| K ₂ O | 3.72 | 3.38 | 4.19 | 3.40 | 2.38 | 4.19 | 4.42 | 2.57 |
| P ₂ O ₅ | 0.201 | 0.210 | 0.325 | 0.262 | 0.246 | 0.243 | 0.148 | 0.140 |
| F | 0.023 | 0.025 | – | – | 0.051 | 0.034 | 0.054 | 0.068 |
| CO ₂ | – | – | – | – | 0.01 | – | < 0.01 | 0.01 |
| C | – | – | – | – | < 0.005 | – | 0.026 | 0.060 |
| S | – | – | – | – | < 0.005 | – | < 0.005 | 0.209 |
| H ₂ O ⁺ | 0.37 | LOI 0.61 | LOI 0.56 | LOI 0.41 | 0.40 | 0.25 | 0.37 | 0.61 |
| H ₂ O ⁻ | < 0.05 | 0.08 | 0.10 | 0.05 | 0.10 | 0.12 | 0.07 | 0.07 |
| Total | 99.81 | 99.30 | 99.26 | 99.28 | 99.21 | 99.34 | 99.39 | 97.75 |

cross-cutting the mylonitic foliation can be observed. The total content of borosilicates is less than 0.5 vol. %. There was found a single grain of a complex rutile–niobian rutile intergrowth, 1.2 mm in diameter, surrounded by biotite. Rutile host with 0.8 wt. % Nb_2O_5 carries unmixed lamellae of niobian–ferroan rutile, which have high-Nb rims with 14.53 wt. % Nb_2O_5 and 5.27 wt. % FeO. The whole-rock value of 3 ppm Nb indicates that niobian rutile must be a very rare accessory.

4.3. Kyanite–garnet–albite–K-feldspar granulite, Běstvína Unit

Samples 5 and 6 are fine-grained rocks from the same outcrop with parallel fabric defined by a weak compositional banding. Garnet is present mainly in felsic patches up to 1.5 cm long, slightly elongated parallel to the foliation. The rest of the rocks is greyish-white and contains small amounts of fine-grained biotite in a felsic matrix. Sample 5 contains approx. 8 vol. % of garnet, 5 % kyanite, 4 % biotite, 30 % albite, 12–15 % K-feldspar and 40 % quartz. Owing to prevalence of albite, the rock is nearly free of mesoperthite. Rutile and apatite are accessories. Sample 8 (KMV98) contains 5 vol. % Grt, 2 % Bt and 1 % Ky. Data for sample 9 (Tab. 1), which is a Bt–Ky–Grt HP/HT “paragneiss” from the Běstvína Unit, are included for comparison. It contains 16 vol. % garnet, 8 % biotite and 10 % kyanite in addition to plagioclase, antiperthite and quartz plus minor pyrrhotite, rutile, apatite and graphite.

5. Whole-rock geochemistry and mineral chemistry

5.1. Whole-rock geochemistry

Some key geochemical parameters are summarised in Tab. 1; complete whole-rock major- and trace-element analyses are presented in Tabs 2 and 3. The felsic gneisses from KHC and calc-alkali felsic granulites from the Běstvína Unit are corundum-normative rocks with alumina saturation index (ASI) 1.10 to 1.26, but the albite granulite sample 5 has ASI = 1.37 and the metasedimentary granulite rich in Grt and Ky, sample 9, has a high ASI value of 2.13. The CIPW norms show that the kyanite–garnet–muscovite felsic gneisses (samples 1 to 3), the foliated leucosome from the migmatite (sample 4) and the albite granulites from the Běstvína Unit (samples 5 and 6) are all identified as albite–K-feldspar–quartz rocks in part chemically corresponding to alkali-feldspar granite. This feature is confirmed by comparison of the calculated plagioclase composition with actual microprobe analyses in Tab. 1. Samples 1, 2 and 4 have high FeOt/MgO ratios between

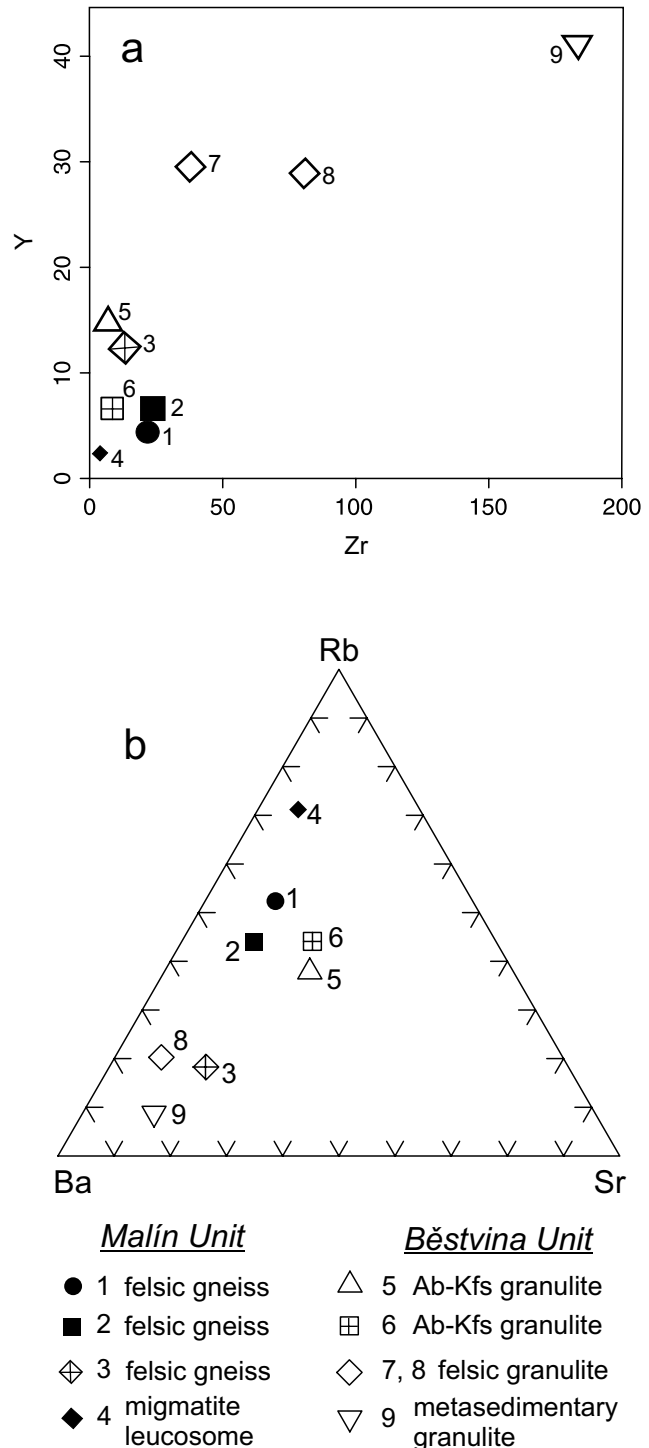


Fig. 4 a – Variations in Zr and Y for the studied samples (ppm); b – Ba, Rb and Sr relations in the studied samples (ppm).

11.1 and 15.0, but sample 3 is different, having $\text{FeOt}/\text{MgO} = 3.25$. Concentrations of certain elements and element/element ratios, such as low FeOt/MnO , Zr/Hf (Tab. 1), Zr and Y (Fig. 4a), high Rb/Sr and Rb/Ba ratios (Fig. 4b), together with low total REE contents (Fig. 5), can be used as valuable petrogenetic indicators.

Tab. 3 Trace element whole-rock analyses of felsic gneisses and granulites (ppm)

| Sample No. | 1 | 2 | 3 | 4 | 5 | 6 | 7 | 8 | 9 |
|------------|-----------------|-------------|--------|---------|---------|---------|---------|--------------|----------------|
| No. | KK30G | KMV43 | KH47A | KH126 | MF153 | MF153A | KK72S | KMV98A | MF7 |
| Locality | Suchdol, quarry | Bohouňovice | Vysoká | Bylanka | Spačice | Spačice | Spačice | Pařížov, dam | Spačice, north |
| Be | < 1 | < 1 | < 1 | < 1 | < 1 | < 1 | | < 1 | < 1 |
| Rb | 90.5 | 67.2 | 106.3 | 115.1 | 124.1 | 110.7 | 130 | 132.4 | 85.0 |
| Sr | 20.6 | 20.5 | 99.7 | 11.6 | 85.1 | 58.4 | 198 | 54.2 | 123.2 |
| Ba | 60 | 67 | 376 | 35 | 119 | 82 | | 467 | 760 |
| Cs | 2.5 | 0.8 | 4.3 | 2.1 | 0.9 | 0.8 | | 0.9 | 0.6 |
| Ni | 0.7 | 1.3 | 3.0 | 1.7 | 63.0 | 9.6 | 8 | 2.9 | 99.9 |
| Co | 0.6 | 0.4 | 0.4 | 0.5 | 3.1 | 2.5 | | 2.5 | 23.6 |
| V | < 8 | < 8 | < 8 | < 8 | 22 | 21 | | 22 | 143 |
| Mo | < 0.1 | < 0.1 | < 0.1 | 0.1 | 11.2 | 0.2 | 1 | 0.2 | 2.9 |
| Sn | 2 | 2 | 4 | 1 | 8 | 10 | < 2 | < 1 | < 1 |
| Cu | 1.8 | 1.5 | 2.2 | 2.9 | 4.5 | 4.4 | 1 | 2.3 | 70.3 |
| Pb | 1.3 | 2.2 | 2.2 | 1.9 | 1.1 | 0.5 | < 2 | 0.8 | 1.3 |
| Zn | 2 | 2 | 10 | 5 | 33 | 32 | 27 | 9 | 92 |
| Ga | 15.9 | 16.8 | 14.2 | 14.1 | 17.0 | 18.4 | | 15.5 | 21.2 |
| Zr | 20.9 | 22.0 | 11.3 | 3.8 | 5.6 | 6.8 | 38 | 81.3 | 183.8 |
| Hf | 1.5 | 1.4 | 0.6 | 0.2 | 0.3 | 0.3 | | 3.0 | 6.1 |
| Nb | 0.4 | 0.6 | 2.8 | 3.0 | 6.7 | 3.0 | 4 | 4.4 | 15.1 |
| Ta | < 0.1 | < 0.1 | 0.5 | 0.1 | 0.2 | 0.2 | | < 0.1 | 0.7 |
| W | < 0.5 | < 0.5 | 0.7 | 0.9 | 2.2 | 1.0 | | < 0.5 | 1.7 |
| Th | 0.2 | 0.4 | 1.1 | 0.9 | 1.4 | 0.4 | | 1.3 | 14.5 |
| U | 1.4 | 0.7 | 2.1 | 5.8 | 1.5 | 0.6 | < 2 | 0.3 | 2.1 |
| La | 1.9 | 2.5 | 4.4 | 1.7 | 11.6 | 4.1 | | 17.5 | 43.8 |
| Ce | 3.3 | 4.8 | 9.1 | 2.7 | 32.4 | 9.4 | | 40.2 | 98.6 |
| Pr | 0.35 | 0.52 | 1.09 | 0.32 | 3.13 | 1.17 | | 4.96 | 9.95 |
| Nd | 1.5 | 1.7 | 4.0 | 1.3 | 13.0 | 4.9 | | 19.6 | 37.4 |
| Sm | 0.37 | 0.40 | 1.29 | 0.27 | 2.79 | 1.09 | | 4.51 | 7.10 |
| Eu | 0.11 | 0.12 | 0.92 | 0.04 | 0.51 | 0.23 | | 0.50 | 1.59 |
| Gd | 0.46 | 0.55 | 1.68 | 0.30 | 2.65 | 1.13 | | 4.34 | 6.84 |
| Tb | 0.12 | 0.15 | 0.39 | 0.07 | 0.50 | 0.21 | | 0.84 | 1.23 |
| Dy | 0.84 | 1.00 | 2.26 | 0.46 | 2.83 | 1.16 | | 4.86 | 7.27 |
| Ho | 0.14 | 0.22 | 0.40 | 0.07 | 0.45 | 0.21 | | 0.99 | 1.42 |
| Er | 0.48 | 0.64 | 1.02 | 0.25 | 1.43 | 0.59 | | 2.94 | 4.16 |
| Tm | 0.10 | 0.13 | 0.14 | 0.04 | 0.22 | 0.10 | | 0.48 | 0.64 |
| Yb | 0.72 | 0.76 | 0.83 | 0.41 | 1.43 | 0.58 | | 2.89 | 4.13 |
| Lu | 0.11 | 0.12 | 0.11 | 0.06 | 0.20 | 0.09 | | 0.41 | 0.61 |
| Y | 4.7 | 6.2 | 12.5 | 2.4 | 14.8 | 6.4 | 29.6 | 29.0 | 41.2 |

Somewhat surprisingly, the garnet–kyanite–muscovite migmatite leucosome (sample 4) is also an albitic rock with several features of highly evolved composition, such as low values of $Zr/Hf = 19$, $FeOt/MnO = 10$ and a low total REE contents. Trace-element data for samples 5 and 6 from the same outcrop in the Běstvina Unit show several geochemical features indicating a highly evolved, probably magmatic protolith. The rock has a low value $Zr/Hf = 18.7$ and rather low $FeOt/MnO$ ratio of 30.2.

5.2. Mineral chemistry

Representative mineral compositions are given in Tabs 4–8.

5.2.1. Garnet

In samples 1 and 2 (fine-grained felsic gneiss), garnet is the only mafic mineral, typically less than 2 mm in diameter. It contains 80.0–82.9 mol. % Alm, 7.9–12.9 % Prp, 4.1–7.8 % Sps, and 0.8–4.0 % Grs (Tab. 4). Widely scattered, coarse relict garnet crystals in the same rock are represented by sample 501 (Tab. 4a) from Bohouňovice (Fig. 6a). The garnet compositional profile (Fig. 6b) exhibits a high Sps content in the central part up to 27.6 mol. %, Grs ~ 0, and Prp of 5.6 to 7.4 % (Fig. 6b). Figure 7 presents comparison of the radiating pattern of quartz–garnet intergrowth in sample 501 and in unmetamorphosed garnetiferous granite. The narrow rim zone of

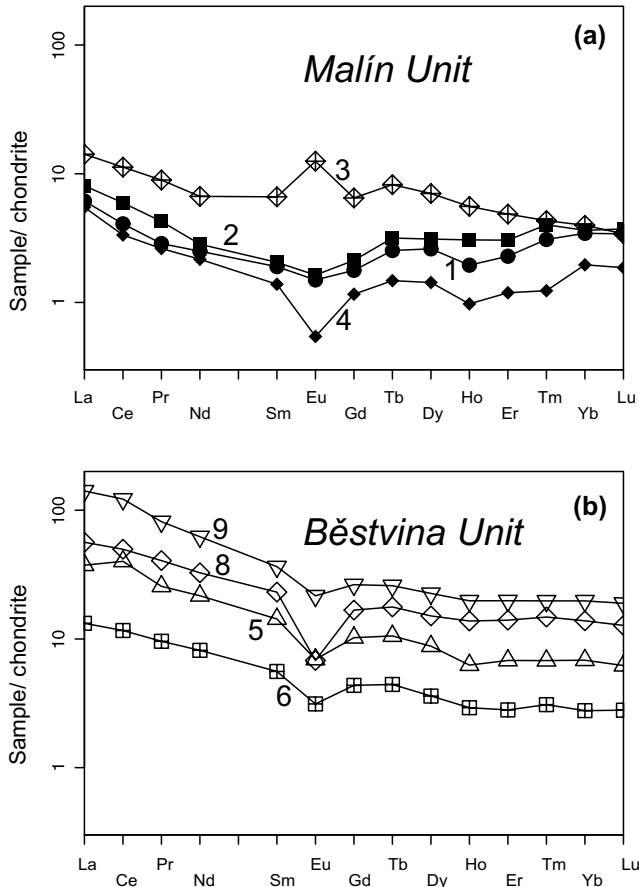
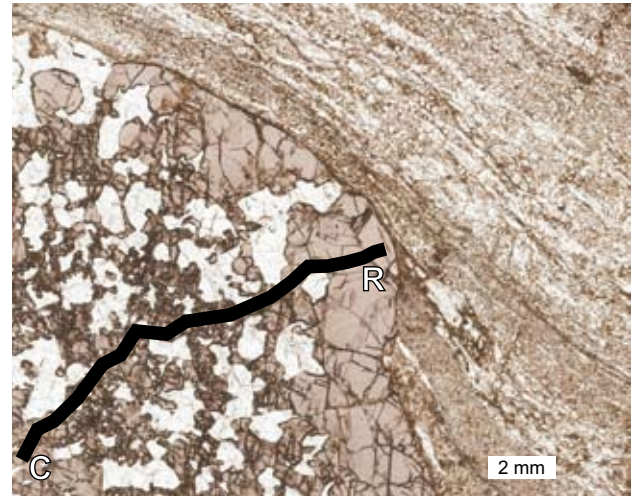


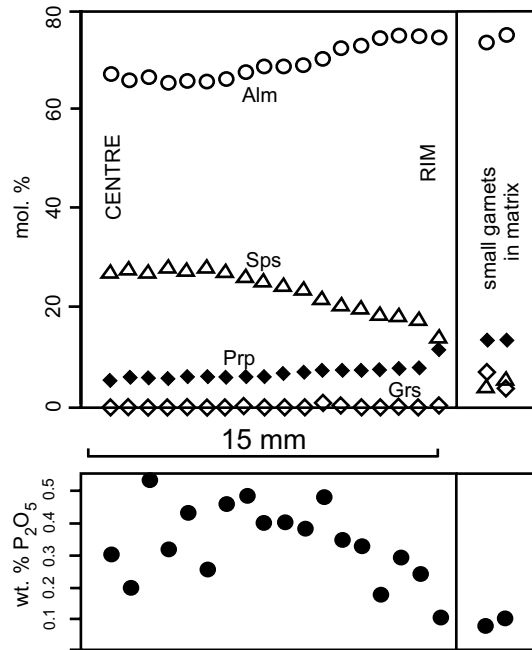
Fig. 5 Chondrite-normalized (Boynton 1984) REE distribution patterns for albite–K-feldspar felsic gneisses (1–3), leucosome of polymetamorphic migmatite (4) (all Malín Unit), felsic albite–K-feldspar (5–6) and calc–alkali granulites (8–9) from the Běstvína Unit.

large relict garnet and small garnet crystals (< 0.2 mm in diameter) in the mylonitic matrix of sample 501 have compositions with 2.0–7.5 mol % Grs, 9.3–13.6 % Prp, and 12.9–3.7 % Sps, which is distinctly different from the composition of the central parts of the large relict garnet (Tab. 4, Fig. 6b). The rim composition of the garnet porphyroclasts probably evolved at a stage of matrix garnet growth or modification via diffusion (M_3), as indicated by the increased Grs and Prp components. Based on the available information, it is uncertain whether the small matrix garnets in samples 1, 2 and 501 represent a pre-metamorphic population with compositions strongly modified by diffusive metamorphic (M_3) re-equilibration, or a new garnet generation produced during the M_3 metamorphism. The source of Mg leading to the increase in Prp in the small garnets in the matrix is uncertain. Possibly a small amount of primary biotite, consumed by Grt-producing reactions, was present.

Minute garnet grains in the biotite-rich laminae in sample 3 contain 83 mol. % Alm, 10.1 % Prp, 4.4 % Sps and 1.7 % Grs (Tab. 4).



(a)



(b)

Fig. 6 a – Relict garnet porphyroclast in mylonitic matrix of kyanite–garnet–muscovite felsic gneiss from Bohouňovice, sample 501; location of compositional profile C–R is indicated by a thick line; **b** – Compositional profile across relict garnet porphyroclast (sample 501); position is indicated in Fig. 6a.

Garnet in leucosome from the Bylanka migmatite (sample 4) forms crystals up to 5 mm in diameter and contains 72.2–76.5 mol. % Alm, 16.2–21.5 % Prp, 3.1–3.5 % Sps, and 2.5–3.1 % Grs. The elevated content of 0.05 to 0.10 wt. % Na_2O (Tab. 4) is interesting as a potential indication of ultra-high pressure conditions. Small garnet in the same sample shows lower Prp and Grs than the large crystal and contains 81.9 mol. % Alm, 12.5 % Prp, 3.7 % Sps, and 1.7 % Grs.

Tab. 4 Chemical composition of garnet (wt. %, apfu and mol. %)

| Sample No. | 1 | 1 | 2 | 2 | 3 | 501 | 501 | 501 | 4 | 4 |
|--------------------------------|--------|--------|--------|--------|-------|--------|-------|-------|-------|-------|
| Analysis No. | 89c* | 96r | 77 | 78 | 41c | 15 int | 19 r | 22 sm | 5r | 2c |
| SiO ₂ | 36.51 | 36.84 | 37.40 | 37.57 | 36.78 | 35.93 | 36.59 | 37.17 | 37.49 | 37.44 |
| TiO ₂ | 0.00 | 0.00 | 0.01 | 0.00 | 0.00 | 0.00 | 0.00 | 0.00 | 0.03 | 0.07 |
| Al ₂ O ₃ | 20.84 | 20.96 | 21.06 | 21.29 | 20.75 | 20.78 | 20.60 | 20.91 | 20.94 | 20.83 |
| Cr ₂ O ₃ | 0.01 | 0.00 | 0.01 | 0.01 | 0.01 | 0.00 | 0.00 | 0.00 | 0.00 | 0.00 |
| FeO ^I | 37.00 | 36.03 | 35.66 | 36.63 | 37.00 | 30.15 | 33.31 | 33.61 | 34.30 | 34.12 |
| MnO | 3.35 | 3.13 | 1.89 | 1.81 | 1.89 | 11.71 | 5.56 | 1.64 | 1.52 | 1.18 |
| MgO | 1.90 | 1.95 | 3.11 | 3.25 | 2.49 | 1.35 | 2.43 | 3.39 | 3.96 | 4.44 |
| CaO | 0.55 | 1.69 | 0.93 | 0.73 | 0.85 | 0.45 | 1.37 | 3.02 | 1.28 | 1.16 |
| Na ₂ O | 0.08 | 0.02 | 0.02 | 0.01 | 0.02 | 0.06 | 0.00 | 0.01 | 0.05 | 0.10 |
| P ₂ O ₅ | 0.28 | 0.14 | – | – | 0.05 | 0.32 | 0.06 | 0.07 | 0.15 | 0.28 |
| Total | 100.52 | 100.76 | 100.09 | 101.30 | 99.84 | 100.75 | 99.92 | 99.82 | 99.72 | 99.62 |
| Number of ions (8 cats) | | | | | | | | | | |
| Si | 2.977 | 2.980 | 3.008 | 2.993 | 2.992 | 2.942 | 2.977 | 2.989 | 3.013 | 3.010 |
| Ti | – | – | 0.001 | – | – | – | – | – | 0.002 | 0.004 |
| Al ^{IV} | 0.023 | 0.020 | 0.000 | 0.007 | 0.008 | 0.058 | 0.023 | 0.011 | 0.000 | 0.000 |
| Al ^{VI} | 1.981 | 1.980 | 1.998 | 1.993 | 1.983 | 1.952 | 1.955 | 1.972 | 1.984 | 1.975 |
| Cr | 0.001 | – | 0.001 | 0.001 | 0.001 | – | – | – | – | – |
| Fe ³⁺ | 0.016 | 0.018 | 0.000 | 0.006 | 0.015 | 0.042 | 0.040 | 0.025 | 0.001 | 0.010 |
| Fe ²⁺ | 2.506 | 2.420 | 2.407 | 2.435 | 2.502 | 2.023 | 2.227 | 2.235 | 2.305 | 2.284 |
| Mn | 0.231 | 0.214 | 0.129 | 0.122 | 0.130 | 0.812 | 0.383 | 0.112 | 0.103 | 0.080 |
| Mg | 0.231 | 0.235 | 0.373 | 0.386 | 0.302 | 0.165 | 0.295 | 0.406 | 0.474 | 0.532 |
| Ca | 0.048 | 0.146 | 0.080 | 0.062 | 0.074 | 0.042 | 0.119 | 0.260 | 0.110 | 0.100 |
| End-member mol. % | | | | | | | | | | |
| Alm | 82.8 | 80.0 | 80.5 | 80.9 | 83.1 | 65.4 | 73.2 | 74.0 | 76.8 | 76.0 |
| Sps | 7.8 | 7.2 | 4.3 | 4.1 | 4.4 | 27.6 | 12.8 | 3.7 | 3.5 | 2.7 |
| Prp | 7.8 | 7.9 | 12.5 | 12.9 | 10.1 | 5.6 | 9.9 | 13.6 | 15.9 | 17.9 |
| Grs | 0.8 | 4.0 | 2.7 | 1.8 | 1.7 | 0.0 | 2.0 | 7.5 | 3.7 | 2.9 |
| Adr | 0.8 | 0.9 | 0.0 | 0.3 | 0.7 | 1.4 | 2.0 | 1.2 | 0.1 | 0.5 |
| Uvr | 0.0 | 0.0 | 0.0 | 0.0 | 0.0 | 0.0 | 0.0 | 0.0 | 0.0 | 0.0 |

* c and r denote core and rim, respectively; int – interior part, sm – small grains in matrix

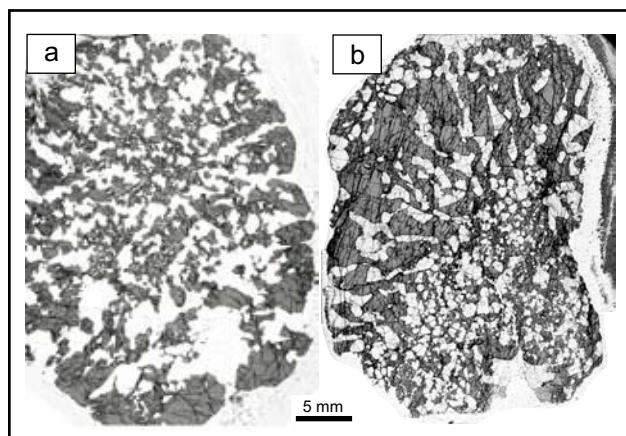


Fig. 7 a – Aggregate of intergrown Alm–Sps garnet and quartz from Ky–Grt–Ms felsic gneiss (sample 2, Bohouňovice); b – Aggregate of intergrown Alm–Sps garnet (Sps up to 13.3 mol. %) and quartz from unmetamorphosed leucogranite dyke crosscutting Sil–Crd migmatite, Zajíčkov near Pelhřimov (Vrána 2005). Note the close similarity in the radiating pattern of quartz grains in garnet.

Garnet in the albitic granulite from the Běstvina Unit (sample 5) contains 57–62 mol. % Alm, 31.5–32.5 % Prp, 3.6–6.6 % Grs. The equant anhedral grains are free of any decompression reaction products. Garnet compositions in all samples are compared in Fig. 8.

5.2.2. Feldspars

Plagioclase from the felsic gneisses contains 5.3–8.0 mol. % anorthite, 91.0–95.5 % albite, and 1.0–2.2 % orthoclase (Tab. 6). The K-feldspar contains 6.0–10.5 mol. % albite, 89.4–94.0 % orthoclase, and up to 0.6 % anorthite (Tab. 7).

5.2.3. Tourmaline

The migmatite leucosome (sample 4) contains two types of tourmaline that are very similar to those in sample 3 from Vysoká (Fig. 9), and an identical type of dumortierite. Ex-

Tab. 4 Chemical composition of garnet (continued)

| Sample No. | 4 | 5 | 5 | 7 | 7 | 8 | 8 | 9 | 9 |
|--------------------------------|--------|--------|--------|-------|-------|--------|--------|--------|--------|
| Analysis No. | 56 | 3c | 4r | 48c | 38r | 72c | 71r | 19c | 29r |
| SiO ₂ | 37.34 | 38.94 | 38.89 | 37.80 | 37.68 | 38.47 | 38.42 | 39.23 | 38.85 |
| TiO ₂ | 0.00 | 0.02 | 0.02 | 0.05 | 0.01 | 0.04 | 0.01 | 0.05 | 0.02 |
| Al ₂ O ₃ | 21.32 | 22.09 | 21.92 | 21.09 | 21.29 | 21.75 | 21.68 | 22.12 | 21.79 |
| Cr ₂ O ₃ | 0.00 | < 0.01 | < 0.01 | 0.00 | 0.02 | 0.01 | 0.03 | < 0.01 | 0.02 |
| FeO ^I | 37.05 | 27.35 | 29.16 | 29.56 | 31.37 | 26.61 | 31.11 | 25.63 | 27.24 |
| MnO | 1.62 | 0.93 | 0.94 | 0.43 | 0.50 | 0.56 | 0.69 | 0.33 | 0.37 |
| MgO | 3.12 | 8.54 | 8.23 | 5.92 | 6.96 | 6.78 | 6.07 | 9.28 | 8.83 |
| CaO | 0.69 | 2.78 | 1.63 | 4.94 | 1.45 | 5.92 | 2.81 | 4.12 | 3.02 |
| Na ₂ O | 0.06 | 0.05 | 0.03 | 0.02 | 0.00 | 0.02 | 0.02 | < 0.01 | < 0.01 |
| P ₂ O ₅ | 0.57 | – | – | 0.10 | 0.03 | – | – | – | – |
| Total | 101.77 | 100.70 | 100.82 | 99.91 | 99.31 | 100.16 | 100.84 | 100.76 | 100.14 |
| Number of ions (8 cats) | | | | | | | | | |
| Si | 2.984 | 2.988 | 2.993 | 2.974 | 2.979 | 2.982 | 2.995 | 2.984 | 2.987 |
| Ti | – | 0.001 | 0.002 | 0.003 | 0.000 | 0.002 | 0.001 | 0.003 | 0.001 |
| Al ^{IV} | 0.016 | 0.012 | 0.007 | 0.026 | 0.021 | 0.018 | 0.005 | 0.016 | 0.013 |
| Al ^{VI} | 1.993 | 1.986 | 1.981 | 1.934 | 1.965 | 1.970 | 1.988 | 1.969 | 1.967 |
| Cr | – | – | – | – | 0.000 | 0.001 | 0.001 | – | 0.001 |
| Fe ³⁺ | 0.007 | 0.011 | 0.017 | 0.056 | 0.031 | 0.024 | 0.009 | 0.025 | 0.036 |
| Fe ²⁺ | 2.470 | 1.744 | 1.860 | 1.889 | 2.043 | 1.701 | 2.019 | 1.605 | 1.715 |
| Mn | 0.110 | 0.060 | 0.062 | 0.029 | 0.043 | 0.037 | 0.046 | 0.021 | 0.024 |
| Mg | 0.372 | 0.977 | 0.945 | 0.694 | 0.820 | 0.783 | 0.705 | 1.052 | 1.012 |
| Ca | 0.059 | 0.229 | 0.135 | 0.416 | 0.123 | 0.494 | 0.235 | 0.336 | 0.249 |
| End-member mol. % | | | | | | | | | |
| Alm | 81.9 | 57.6 | 61.9 | 61.7 | 67.2 | 55.9 | 67.1 | 52.8 | 57.0 |
| Sps | 3.7 | 2.0 | 2.1 | 1.0 | 1.1 | 1.2 | 1.5 | 0.7 | 0.8 |
| Prp | 12.5 | 32.7 | 31.5 | 23.3 | 27.5 | 26.3 | 23.6 | 35.2 | 33.8 |
| Grs | 1.6 | 7.1 | 3.9 | 11.2 | 2.6 | 15.4 | 7.3 | 10.0 | 7.0 |
| Adr | 0.3 | 0.6 | 0.6 | 2.8 | 1.5 | 1.2 | 0.5 | 1.3 | 1.3 |
| Uvr | 0.0 | 0.0 | 0.0 | 0.0 | 0.0 | 0.0 | 0.0 | 0.0 | 0.1 |

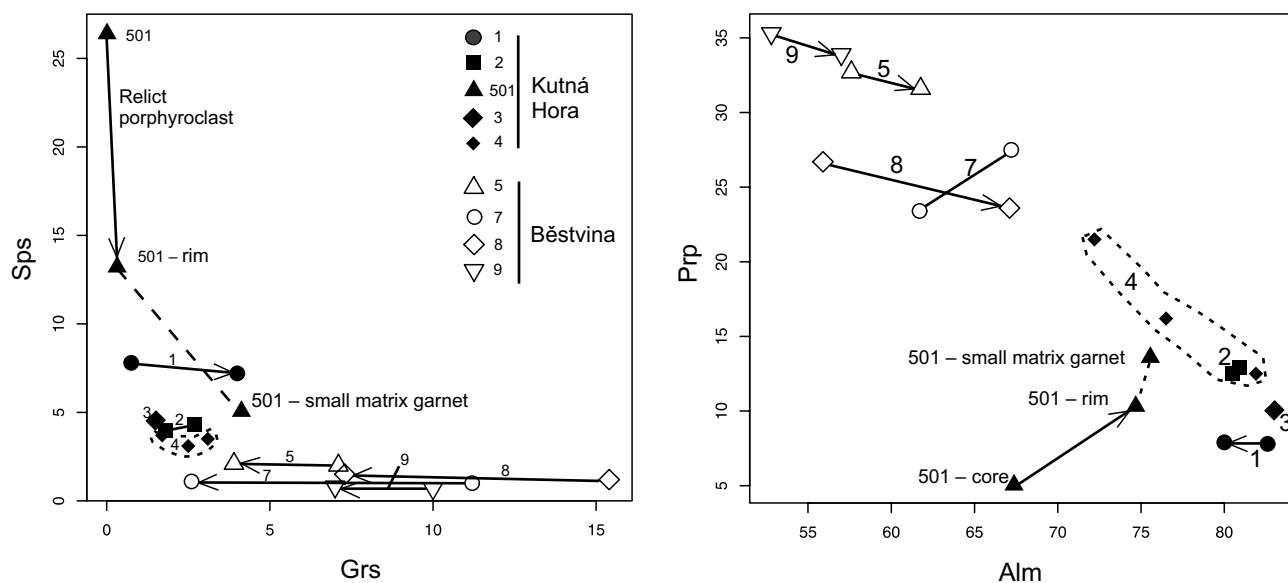


Fig. 8 Comparison of the garnet compositions for samples of kyanite–garnet–muscovite felsic gneisses from the vicinity of Kutná Hora (samples 1–4, and 501) with garnets from granulites of the Běstvína Unit (samples 5, 7–9). Sample numbers and rock types are given in Tab. 1.

Tab. 5 Chemical composition of biotite (wt. % and apfu)

| Sample No. | 3 | 501 | 4 | 5 | 7 | 8 | 9 |
|--------------------------------|-------|-------|-------|-------|-------|-------|-------|
| Anal. No. | 39b | 23 | 50 | 16 | 37 | 75 | 22 |
| SiO ₂ | 34.58 | 34.45 | 35.26 | 37.56 | 37.16 | 36.74 | 37.96 |
| TiO ₂ | 3.45 | 0.24 | 2.60 | 4.42 | 4.14 | 3.94 | 4.42 |
| Al ₂ O ₃ | 19.55 | 20.95 | 20.11 | 16.89 | 16.93 | 18.30 | 17.78 |
| Cr ₂ O ₃ | 0.03 | 0.02 | 0.02 | 0.06 | 0.10 | 0.05 | 0.07 |
| FeO | 22.74 | 20.48 | 20.54 | 13.77 | 12.09 | 14.82 | 10.81 |
| MnO | 0.09 | 0.10 | 0.18 | 0.08 | bd | bd | 0.04 |
| MgO | 5.71 | 7.95 | 7.21 | 12.96 | 14.59 | 12.12 | 15.39 |
| CaO | 0.07 | 0.07 | bd | bd | 0.04 | bd | bd |
| BaO | bd | 0.03 | bd | – | – | – | – |
| Na ₂ O | 0.09 | 0.08 | 0.08 | 0.06 | 0.08 | 0.11 | 0.14 |
| K ₂ O | 8.77 | 9.09 | 9.08 | 9.73 | 9.16 | 9.43 | 9.43 |
| P ₂ O ₅ | 0.02 | 0.04 | 0.04 | – | bd | – | – |
| ZnO | 0.20 | – | 0.05 | – | – | – | – |
| F | 0.07 | bd | bd | – | – | – | – |
| Cl | 0.01 | 0.01 | 0.03 | – | – | – | – |
| Total | 95.38 | 93.51 | 95.20 | 95.53 | 94.29 | 95.51 | 96.04 |
| Number of ions 24 (O,OH,F) | | | | | | | |
| Si | 5.340 | 5.363 | 5.143 | 5.551 | 5.508 | 5.447 | 5.485 |
| Ti | 0.401 | 0.028 | 0.312 | 0.491 | 0.462 | 0.439 | 0.480 |
| Al ^{IV} | 2.660 | 2.637 | 2.857 | 2.449 | 2.492 | 2.553 | 2.515 |
| Al ^{VI} | 0.899 | 1.207 | 0.922 | 0.493 | 0.466 | 0.644 | 0.513 |
| Cr | 0.004 | 0.003 | 0.003 | 0.007 | 0.012 | 0.006 | 0.008 |
| Fe ²⁺ | 2.937 | 2.666 | 2.739 | 1.702 | 1.499 | 1.837 | 1.306 |
| Mn | 0.012 | 0.013 | 0.024 | 0.010 | – | – | 0.005 |
| Mg | 1.314 | 1.845 | 1.714 | 2.855 | 3.224 | 2.678 | 3.315 |
| Ca | 0.012 | 0.012 | – | – | 0.006 | – | – |
| Ba | – | 0.002 | – | – | – | – | – |
| Na | 0.027 | 0.024 | 0.025 | 0.017 | 0.023 | 0.032 | 0.039 |
| K | 1.728 | 1.805 | 1.846 | 1.834 | 1.723 | 1.783 | 1.738 |
| Zn | 0.023 | – | – | – | – | – | – |
| F | 0.034 | – | – | – | – | – | – |
| Cl | 0.003 | – | – | – | – | – | – |

cept for differences in the Ti content, the composition of the two types of tourmaline in sample 3 is very similar (Tab. 8, Fig. 10) and corresponds to dravite–schorl (Selway and Novák 1997), with Mg prevailing over Fe. Our samples of felsic gneisses contain no evidence of primary tourmaline.

5.2.4. Dumortierite

Compared to the composition of igneous dumortierite in common pegmatites (Fiala 1954; Losert 1956a; Cempírek and Novák 2006), the metamorphic dumortierite of the studied samples (Tab. 8, Fig. 9) shows somewhat higher Ti, Fe and Mg contents (0.20–0.83 wt. % TiO₂, 1.02–1.20 % MgO and 0.23–0.25 % FeOt).

6. Geothermobarometry

Pressure and temperature calculations were performed using the garnet–alumina silicate–plagioclase (GASP)

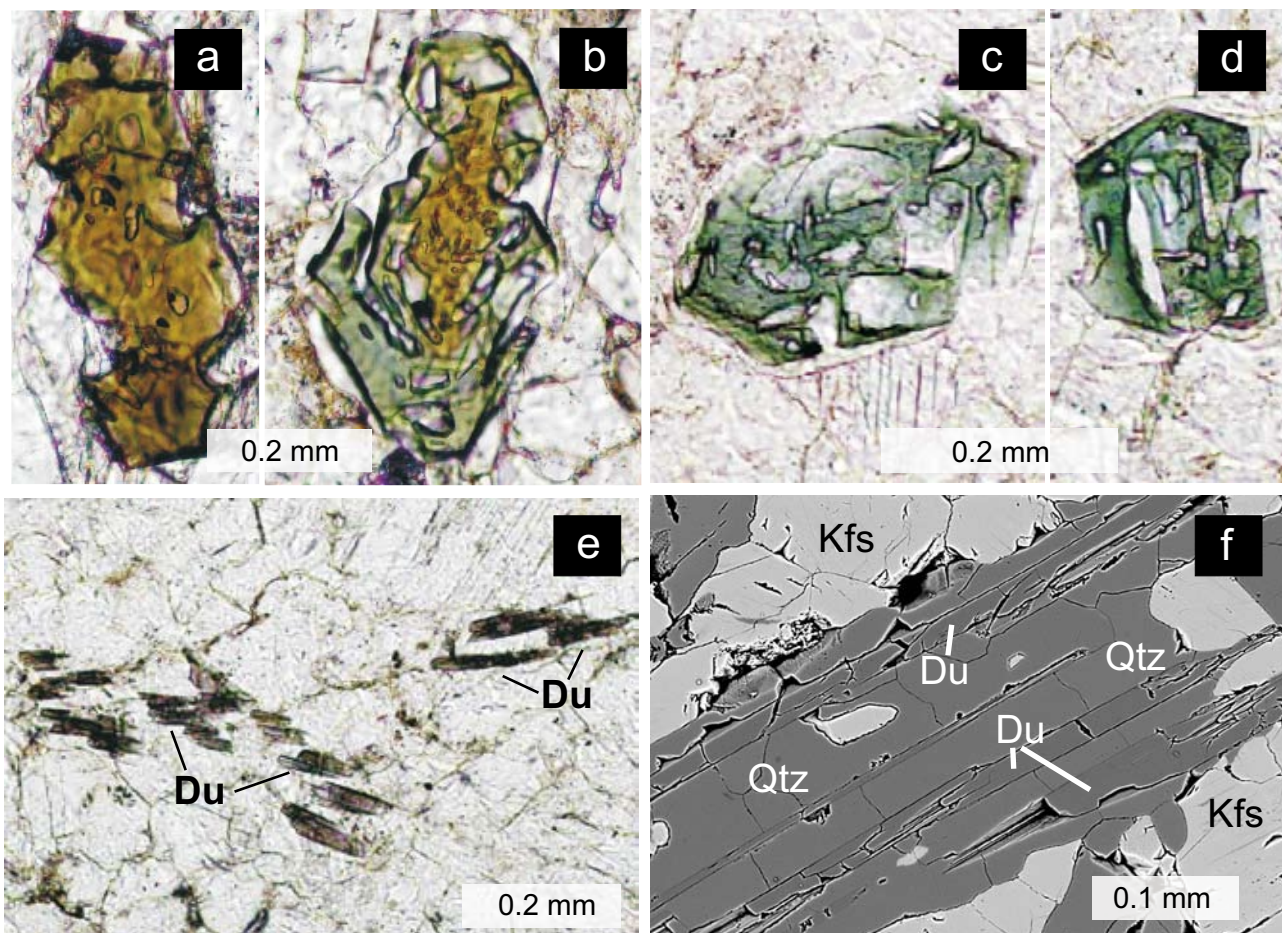
barometer of Koziol and Newton (1988). Garnet–biotite thermometry was carried out using the methods of Ferry and Spear (1978), Indares and Martignole (1985) and Williams and Grambling (1990). The results of P-T calculations are presented in Fig. 11. The set of Excel spreadsheet programs (Reche and Martinez 1996) was used for P-T calculations. The equation by Williams and Grambling (1990) was proposed for medium-grade Grt–Bt pairs, in which Grt has $X < 0.1$ Ca, biotite contains less than 2.4 wt. % TiO₂ and 10 % of total iron in biotite is recalculated to Fe₂O₃. In our sample set, especially in samples of the HP/HT granulites from the Běstvina Unit,

⇒

Fig. 9 Microstructures of tourmaline (a–d) and dumortierite (e–f) in albite–K-feldspar felsic gneiss, sample 3, Vysoká; **a** – Early khaki tourmaline; **b** – Khaki tourmaline core overgrown by light blue–green subhedral tourmaline; **c–d** – Subhedral light blue–green tourmaline with quartz inclusions and narrow rims of quartz; **e** – Violet dumortierite (Du) in quartz–feldspar matrix, (a to e – transmitted light photomicrographs with single polarizer), **f** – Quartz–dumortierite intergrowth, BSE image. See explanation in text.

Tab. 6 Chemical composition of plagioclase (wt. % and apfu)

| Sample No. | 1 | 2 | 3 | 501 | 4 | 5 | 5 | 7 | 8 | 9 | 9 |
|--------------------------------|--------|--------|-------|-------|--------|--------|--------|-------|--------|--------|--------|
| Analysis No. | 65 | 81 | 8b | 26 | 57 | 5 | 6 | 164 | 73 | 25 | 26 |
| SiO ₂ | 67.65 | 66.68 | 66.70 | 65.71 | 67.68 | 66.69 | 66.78 | 63.98 | 65.06 | 65.11 | 65.66 |
| Al ₂ O ₃ | 20.17 | 20.98 | 20.53 | 21.10 | 20.77 | 21.01 | 21.06 | 22.29 | 22.14 | 22.08 | 21.84 |
| FeOt | bd | 0.24 | 0.01 | 0.02 | bd | 0.01 | bd | 0.04 | bd | bd | bd |
| CaO | 1.09 | 1.69 | 1.05 | 1.89 | 0.84 | 1.75 | 1.86 | 3.66 | 3.20 | 3.22 | 2.82 |
| Na ₂ O | 10.64 | 10.62 | 11.08 | 10.62 | 11.52 | 10.62 | 10.44 | 8.96 | 9.73 | 9.91 | 9.93 |
| K ₂ O | 0.39 | 0.26 | 0.15 | 0.17 | 0.17 | 0.24 | 0.30 | 0.50 | 0.37 | 0.34 | 0.26 |
| BaO | – | 0.11 | bd | bd | bd | – | – | – | – | – | – |
| SrO | – | – | 0.03 | – | 0.05 | – | – | – | – | – | – |
| PbO | – | – | 0.05 | – | bd | – | – | – | – | – | – |
| P ₂ O ₅ | 0.10 | 0.24 | 0.15 | 0.05 | 0.28 | 0.06 | 0.10 | 0.02 | bd | 0.07 | 0.03 |
| Total | 100.04 | 100.82 | 99.75 | 99.56 | 101.31 | 100.38 | 100.54 | 99.45 | 100.50 | 100.73 | 100.54 |
| Number of ions (5 cats) | | | | | | | | | | | |
| Si | 2.970 | 2.916 | 2.931 | 2.899 | 2.927 | 2.919 | 2.923 | 2.850 | 2.856 | 2.850 | 2.880 |
| Al | 1.050 | 1.081 | 1.063 | 1.093 | 1.059 | 1.084 | 1.087 | 1.171 | 1.145 | 1.139 | 1.129 |
| Fe ²⁺ | 0.000 | 0.009 | 0.000 | 0.001 | – | 0.000 | – | 0.001 | – | – | – |
| Ca | 0.050 | 0.079 | 0.049 | 0.090 | 0.039 | 0.082 | 0.087 | 0.175 | 0.151 | 0.151 | 0.133 |
| Na | 0.910 | 0.900 | 0.944 | 0.908 | 0.966 | 0.901 | 0.886 | 0.774 | 0.828 | 0.841 | 0.845 |
| K | 0.020 | 0.015 | 0.008 | 0.010 | 0.009 | 0.013 | 0.017 | 0.028 | 0.021 | 0.019 | 0.015 |
| P | – | – | 0.006 | – | 0.010 | – | – | – | – | – | – |
| Ab | 92.5 | 91.0 | 94.0 | 90.2 | 95.0 | 90.4 | 89.5 | 79.2 | 82.9 | 83.2 | 85.2 |
| An | 5.3 | 8.0 | 5.0 | 8.9 | 4.0 | 8.2 | 8.8 | 17.9 | 15.1 | 14.9 | 13.4 |
| Or | 2.2 | 1.0 | 1.0 | 0.9 | 1.0 | 1.3 | 1.7 | 2.9 | 2.1 | 1.9 | 1.5 |



Tab. 7 Chemical composition of K-feldspar and muscovite (wt. % and apfu)

| Mineral Sample Analysis No. | Kfs 2 84 | Kfs 3 13b | Kfs 501 27 | Kfs 7 165 | Mineral Sample Analysis No. | Ms II 1 74 | Ms II 2 82 | Ms II 3 7b | Ms II 501 24 | Ms I 4 7 |
|-----------------------------------|----------------|-----------------|------------------|-----------------|-------------------------------------|------------------|------------------|------------------|--------------------|----------------|
| SiO ₂ | 64.67 | 64.37 | 64.94 | 64.32 | SiO ₂ | 46.31 | 46.69 | 47.52 | 47.45 | 48.09 |
| TiO ₂ | – | – | – | – | TiO ₂ | 1.01 | 0.37 | 1.22 | 0.35 | 0.54 |
| Al ₂ O ₃ | 18.59 | 18.44 | 18.45 | 18.70 | Al ₂ O ₃ | 34.34 | 34.25 | 32.58 | 34.71 | 33.15 |
| Cr ₂ O ₃ | – | – | – | – | Cr ₂ O ₃ | 0.01 | 0.00 | 0.00 | 0.01 | 0.01 |
| FeOt | 0.24 | 0.00 | 0.00 | 0.01 | FeOt | 1.34 | 1.49 | 1.26 | 1.14 | 1.42 |
| MnO | – | – | – | – | MnO | 0.00 | 0.01 | 0.01 | 0.01 | 0.01 |
| MgO | – | – | – | – | MgO | 0.53 | 1.01 | 1.28 | 0.93 | 1.38 |
| CaO | 0.00 | 0.00 | 0.05 | 0.11 | CaO | 0.00 | 0.02 | 0.00 | 0.00 | 0.07 |
| SrO | – | 0.09 | – | – | Na ₂ O | 0.51 | 0.55 | 0.37 | 0.41 | 0.70 |
| Na ₂ O | 0.63 | 1.01 | 1.40 | 1.53 | K ₂ O | 10.37 | 10.46 | 10.55 | 11.23 | 10.04 |
| K ₂ O | 15.70 | 14.88 | 14.66 | 14.27 | BaO | – | – | – | 0.10 | – |
| BaO | 0.03 | 0.10 | 0.01 | – | F | – | – | 0.21 | 0.04 | 0.09 |
| P ₂ O ₅ | 0.16 | 0.32 | 0.39 | 0.02 | Cl | – | – | 0.01 | 0.00 | 0.00 |
| Total | 99.99 | 99.20 | 99.90 | 98.96 | Total | 94.42 | 94.85 | 95.10 | 96.38 | 95.54 |
| Number of ions based on 5 cations | | | | | Number of ions based on 24 (O,OH,F) | | | | | |
| Si | 2.993 | 2.981 | 3.002 | 2.978 | Si | 6.217 | 6.245 | 6.352 | 6.261 | 6.371 |
| Al ^{IV} | 1.014 | 1.007 | 1.005 | 1.024 | Al ^{IV} | 1.783 | 1.755 | 1.648 | 1.739 | 1.629 |
| Al ^{VI} | – | – | – | – | Al ^{VI} | 3.650 | 3.645 | 3.486 | 3.660 | 3.548 |
| Ti | – | – | – | – | Ti | 0.102 | 0.037 | 0.123 | 0.035 | 0.054 |
| Cr | – | – | – | – | Cr | 0.001 | 0.000 | – | 0.001 | 0.001 |
| Fe ²⁺ | 0.009 | 0.000 | 0.000 | 0.000 | Fe ²⁺ | 0.150 | 0.167 | 0.141 | 0.126 | 0.157 |
| Mn | – | – | – | – | Mn | 0.000 | 0.001 | 0.001 | 0.001 | 0.001 |
| Mg | – | – | – | – | Mg | 0.106 | 0.201 | 0.255 | 0.183 | 0.273 |
| Ca | 0.000 | 0.000 | 0.002 | 0.005 | Ca | 0.000 | 0.003 | – | – | 0.010 |
| Na | 0.057 | 0.091 | 0.125 | 0.138 | Na | 0.133 | 0.143 | – | 0.107 | 0.180 |
| K | 0.927 | 0.879 | 0.865 | 0.845 | K | 1.776 | 1.785 | – | 1.890 | 1.697 |
| P | – | 0.012 | – | – | F | – | – | 0.089 | 0.017 | 0.038 |
| Or | 94.0 | 94.0 | 87.2 | 85.1 | Cl | – | – | 0.002 | – | 0.000 |
| Ab | 6.0 | 5.0 | 12.6 | 13.9 | | | | | | |
| An | 0.0 | 1.0 | 0.2 | 0.5 | | | | | | |

the interpretation of the geothermometric calculations is difficult, because of the relatively extreme conditions of metamorphism. Garnet in samples 5 to 9 has $X < 0.1$ Ca (with one exception) and contains very low amount of MnO. Alcock (1996) presented data indicating that the effect of the grossular content on the Fe-Mg miscibility in Grt and Bt is small and is offset by other variables. Rather high Ti content in biotite, near 4 wt. %, may represent a deviation from biotite compositions used by Williams and Grambling (1990). Ilmenite in granulites from the Běstvína Unit is free of unmixed hematite and the FeO and TiO₂ ratios indicate minimal Fe³⁺ in solid solution. Some of the felsic granulite samples contain accessory graphite. These features show that the studied sample set equilibrated at lower oxygen fugacity compared to the samples studied by Williams and Grambling (1990). Consequently, correction of biotite composition for a presumed Fe³⁺ content was omitted. The calculated Grt–Bt temperature estimates using the Ferry and Spear (1978) thermometer are approximately by 50 °C lower

than the values calculated with the thermometer of Williams and Grambling (1990). The difference between values for garnet core and garnet rim (using the same biotite composition) was used as a criterion of secondary importance, resting on the assumption that the difference in calculated temperatures for core and rim, respectively, should not be high. The temperatures calculated with the thermometer of Indares and Martignole (1985) are unrealistically low (by as much as 150 °C lower) than data obtained following the procedure of Williams and Grambling (1990). The calculated pressure-temperature data are plotted in Fig. 11, arbitrarily with T uncertainty of 50 °C and P of 0.15 GPa, which are near to a minimal theoretical error following from the character of the thermodynamic data (Williams and Grambling 1990). The true uncertainty in temperature estimate is unknown due to several factors, including the possibility of partial re-equilibration via Grt–Bt ion exchange.

Among samples from the Běstvína Unit, samples 5 and 9 can be used for geobarometric calculations. By using these

Tab. 8 Chemical composition of tourmaline and dumortierite

| Sample Mineral Anal. No. | 3 | | | 4 | |
|-------------------------------------|-----------|-------------|-----------|-------------|------------|
| | Tour I 1b | Tour II 23a | Tour I 15 | Dumort. 10b | Dumort. 58 |
| SiO ₂ | 37.15 | 36.78 | 37.04 | 31.79 | 31.51 |
| TiO ₂ | 0.94 | 0.15 | 1.11 | 0.20 | 0.83 |
| Al ₂ O ₃ | 33.67 | 35.18 | 33.59 | 59.31 | 58.72 |
| B ₂ O ₃ * | 10.78 | 10.81 | 10.83 | 5.90 | 5.90 |
| Cr ₂ O ₃ | 0.01 | 0.00 | 0.01 | 0.00 | 0.00 |
| V ₂ O ₃ | 0.03 | 0.01 | 0.02 | 0.00 | 0.03 |
| FeO | 6.50 | 6.58 | 6.80 | 0.23 | 0.25 |
| MnO | 0.00 | 0.00 | 0.02 | 0.02 | 0.02 |
| MgO | 5.93 | 5.59 | 6.18 | 1.20 | 1.02 |
| CaO | 0.15 | 0.15 | 0.17 | 0.02 | 0.00 |
| Na ₂ O | 2.23 | 2.35 | 2.41 | 0.01 | 0.03 |
| K ₂ O | 0.07 | 0.03 | 0.06 | 0.02 | 0.01 |
| P ₂ O ₅ | 0.00 | 0.00 | 0.08 | 0.07 | 0.00 |
| ZnO | 0.12 | 0.12 | 0.12 | 0.03 | 0.00 |
| H ₂ O* | 3.71 | 3.73 | 3.74 | – | – |
| F | 0.03 | 0.00 | 0.00 | 0.05 | 0.07 |
| Cl | – | – | 0.01 | 0.00 | 0.01 |
| -F eq. | 0.01 | – | – | 0.02 | 0.03 |
| Total | 101.30 | 101.48 | 102.19 | 98.83 | 98.37 |
| Number of ions based on 31 (O,OH,F) | | | | 18 (O,OH) | |
| Si | 5.987 | 5.914 | 5.942 | 3.000 | 3.000 |
| Ti | 0.114 | 0.018 | 0.134 | 0.014 | 0.060 |
| Al | 6.396 | 6.666 | 6.350 | 6.595 | 6.590 |
| B* | 3.000 | 3.000 | 3.000 | 1.000 | 1.011 |
| Cr | 0.001 | – | 0.001 | – | – |
| V | 0.004 | 0.001 | 0.003 | – | 0.002 |
| Fe ²⁺ | 0.876 | 0.885 | 0.912 | 0.018 | 0.020 |
| Mn | – | – | 0.003 | 0.002 | 0.002 |
| Mg | 1.425 | 1.340 | 1.478 | 0.169 | 0.145 |
| Ca | 0.026 | 0.026 | 0.029 | 0.002 | – |
| Na | 0.697 | 0.733 | 0.750 | 0.001 | 0.006 |
| K | 0.014 | 0.006 | 0.012 | 0.001 | 0.001 |
| P | – | – | – | 0.017 | – |
| Zn | 0.014 | 0.014 | 0.014 | 0.002 | – |
| Total | 18.554 | 18.603 | 18.628 | 10.821 | 10.837 |
| F | – | – | – | 0.016 | 0.022 |

* – B₂O₃ in tourmaline and dumortierite and H₂O in tourmaline calculated from stoichiometry (Grew 1996)

samples we avoid problems with unmixed feldspars (mesoperthite), which is usually the main feldspar in felsic granulites. Owing to its rather sodic whole-rock composition, the sample 5 is dominated by albite. Sample 9 contains some antiperthite, but plagioclase is the most common feldspar.

On the other hand, sample 4 – the polymetamorphic leucosome – contains no mineral assemblage suitable for temperature calculation for the M₂ stage: biotite replacing garnet or muscovite I at margins is interpreted as belonging to the M₃ assemblage. Consequently, the pressure data for sample 4 are plotted somewhat arbitrarily at T = 800 °C, with reference to temperature calculated on another migmatite sample from the same Malín Unit (Nahodilová et al. 2006).

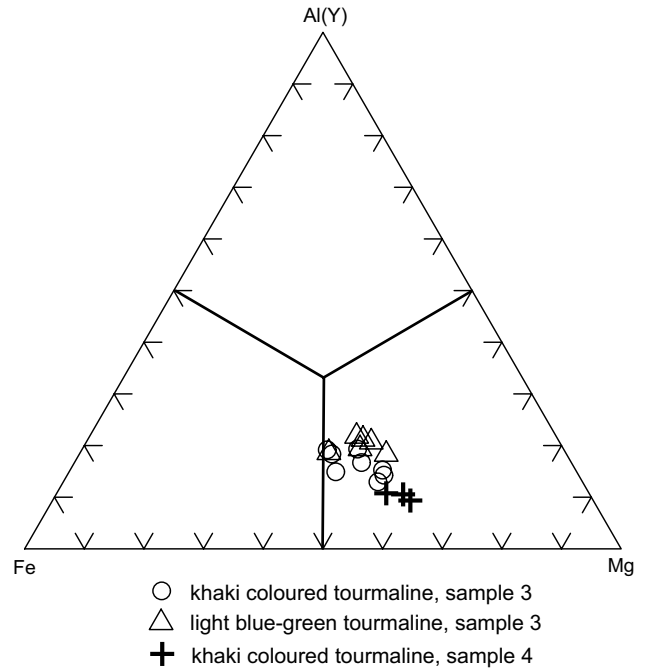
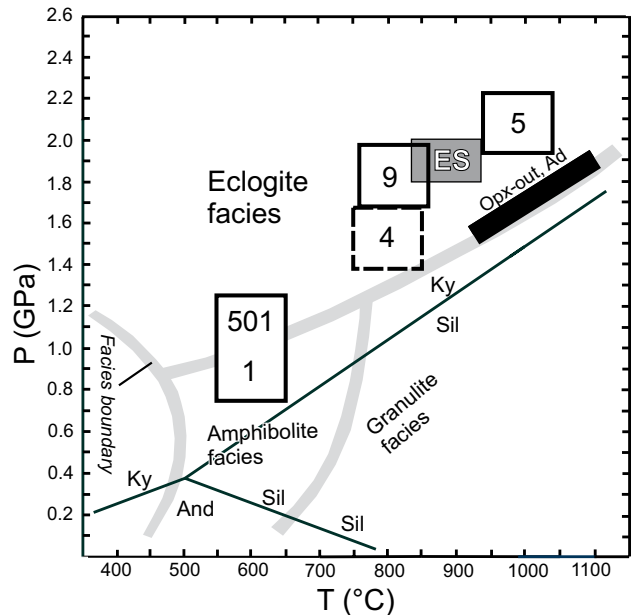

Fig. 10 Tourmaline composition in Fe–Mg–Al(Y) diagram.


Fig. 11 Calculated P–T equilibration conditions for the granulites (samples 5 and 9, Spáčice, Běstvina Unit), the polymetamorphic leucosome from migmatite (sample 4, Malín Unit), and the felsic gneiss (samples 1 and 501, Malín Unit). Data for eclogite of tholeiitic composition from Spáčice village (grey rectangle labelled ES), are from Medaris et al. (2006). The Opx-out curve for adamellite composition (bold contour) is from Green and Lambert (1965). Metamorphic facies fields are from Spear (1993). The calculated pressures and temperatures are plotted with arbitrary errors following from thermodynamic data (temperature \pm 50 °C, pressure 0.15 GPa). True errors are not defined; see text for explanation.

6.1. Data for individual metamorphic events

Event M₁. The calculated P-T conditions for albite–K-feldspar Bi–Ky–Grt granulite, sample 5, correspond to T = 989–980 °C (Williams and Grambling 1990) or 933–872 °C (Ferry and Spear 1978), and P = 1.8–2.1 GPa (Fig. 11).

Calc-alkali Ky–Grt granulites of granite composition in the Běstvína Unit yielded metamorphic conditions of T = 840–920 °C and P = 1.8–2.2 GPa, corresponding to eclogite-facies conditions outside the orthopyroxene stability field (Vrána et al. 2005). The newly obtained information on samples 5 and 6 shows that some albite–K-feldspar rocks with advanced geochemical fractionation endured the HP/HT eclogite-facies conditions, together with the prevailing granulitic rocks of calc-alkali granite composition in the Běstvína Unit.

Nahodilová et al. (2006) calculated for the HP/HT stage of the Běstvína felsic granulite peak P-T conditions of 831 ± 53 °C and 1.65 ± 0.18 GPa, followed by retrogression at 705 ± 97 °C and 1.4 ± 0.2 GPa, using the average P-T method (Powell et al. 1998) and different samples. The results suggest retrogression at relatively high pressure in the kyanite stability field.

Event M₂. The pressure 1.6 GPa calculated for sample 4, leucosome from the Bylanka brook migmatite, is interpreted as relating to the original HP anatectic mineral assemblage. The fact that the leucosome in sample 4 exhibits effects of superimposed penetrative shearing and partial amphibolite-facies recrystallization with newly formed fine-grained muscovite, comparable to D₃/M₃ in felsic gneiss samples 1, 2 and 501, proves that the high-pressure migmatitic assemblage in sample 4 pre-dated the D₃/M₃ event.

Nahodilová et al. (2006) estimated the maximum P-T conditions using the Ky–Grt–Ms–Kfs–Ab–Qtz assemblage in the Malín and Běstvína kyanite-bearing migmatites (M₂?) at 875 ± 95 °C and 1.56 ± 0.14 GPa using the average P-T method (Powell et al. 1998). The data for MP/LT retrogression calculated by Nahodilová et al. (2006) from the matrix biotite, garnet rims and the recrystallized grains of plagioclase, K-feldspar and quartz yielded P-T conditions of 712 ± 39 °C and 1.06 ± 0.18 GPa, which could be compared with the event M₃. The values calculated for the M₂ event in HP migmatites of the Malín Unit can be compared with P-T data obtained for a migmatitic gneiss from the Běstvína Unit (P = 1.4 GPa, T = 660 °C: Vrána et al. 2005).

Event M₃. The Ky–Grt–Ms–Kfs–Ab–Qtz assemblage in the felsic gneiss samples 1, 2 and in the matrix of sample 501 (Bohouňovice and Suchdol) yield an M₃ pressure estimate of 0.9 to 1.2 GPa using the GASP barometry according to Koziol and Newton (1988). Temperature estimate in sample 501, based on the garnet–biotite thermometer of Williams and Grambling (1990) is

730 °C. This rather high value, given the abundance of muscovite, prompted checking muscovite stability field in this sample with the THERMOCALC 3.30 (Powell et al. 1998) pseudosection. Muscovite stability field in the rock of given composition extends up to c. 750 °C at pressure of 1.1 GPa. However, there are some doubts concerning equilibrium between rare biotite and matrix garnet. The equilibration conditions correspond to amphibolite-facies at increased pressure. During the M₃ event, newly formed, fine-grained, syn-foliation muscovite and kyanite crystallized in the country rocks involved in the regional shearing and re-equilibration.

6.2. Comparison of felsic KHC gneisses with felsic granulites from the Běstvína Unit

The kyanite–garnet felsic gneisses from the Malín Unit (KHC) (samples 1 and 2) show geochemical characteristics comparable to unmetamorphosed, highly evolved albite leucogranites worldwide. New trace-element data for samples 5 and 6 (Tab. 3) from the Běstvína Unit, resembling somewhat those for samples 1 and 2 from the Malín Unit, show several geochemical features indicating an evolved, probably magmatic protolith. On the other hand, the albite granulites (samples 5 and 6) differ from the calc-alkali leucogranitic–granitic granulites dominating in the Běstvína Unit, (Fiala et al. 1987; Vrána et al. 2005). These felsic calc-alkali granulites, represented by samples 7 and 8, have equilibrated under eclogite-facies conditions (Vrána et al. 2005). Samples 5 and 6 exhibit relatively high Rb/Sr and Rb/Ba ratios (Fig. 4b), low Zr and Y contents (Fig. 4a) and low total REE contents. However, the overall shapes of the REE patterns are more similar to those of the calc-alkali felsic granulites (sample 8) and the metasedimentary granulite rich in Grt and Ky (sample 9) (Fig. 5), rather than to the felsic gneisses from the Malín Unit. The compositional differences between garnets from albite–K-feldspar felsic gneisses from the KHC and the samples of HT/HP granulites from the Běstvína Unit can be seen in Fig. 8. The high contents of Prp and Grs in garnet from the Běstvína granulites greatly exceed the contents in garnet from the KHC rocks and indicate notably higher P-T conditions for the Běstvína granulites (Fig. 11).

7. Discussion

7.1. Geochemical and mineralogical implications for the protolith of felsic gneisses

There are several whole-rock compositional features indicating that the protoliths of the felsic gneisses from

the Malín Unit were highly fractionated magmatic rocks, namely: high Rb/Sr and Rb/Ba ratios (Fig. 4b), low Zr/Hf ratios (~ 14), low Zr and Y contents (Fig. 4a), low FeOt/MnO ratios (~ 14), and low total REE contents (10–14 ppm) (Tab. 1). Compared to these extreme values, ordinary calc-alkali granitic rocks have Zr/Hf ratios near 30, FeOt/MnO ratios near 50 and total REE contents near 100. Concentrations of certain elements and element/element ratios, such as low FeOt/MnO, Zr/Hf (Tab. 1), Zr and Y (Fig. 4a), high Rb/Sr and Rb/Ba ratios (Fig. 4b), together with low total REE contents prove conclusively that the felsic gneisses were derived by metamorphism of leucogranitic rocks crystallized from highly evolved magmas. The geochemically evolved character of granites is usually shown by high contents of rare elements (Rb, Li, Cs, Sn, Nb, Ta) and strongly depleted REE (Breiter and Scharbert 1998; Černý and Ercit 2005). In contrast, in felsic gneisses the evolved character is manifested by element/element ratios and low to very low contents of rare elements. Chondrite-normalized REE patterns (Fig. 5) show that samples 1 and 2 have only a weak negative Eu anomaly. The protolith for sample 3 from Vysoká is not identified. However, it is different from the protolith for samples 1 and 2 as indicated by differences in FeOt/MgO and FeOt/MnO values, REE characteristics (Fig. 5) and minor element data. The granulite samples 7 and 8 from the Běstvína Unit come near to values similar to ordinary calc-alkali granite.

In peraluminous granites the Zr/Hf ratios tend to be close to the chondritic value (~ 36) (Dostal and Chatterjee 2000). According to Linnen and Keppler (2002) partition coefficients of Zr and Hf between zircon and peraluminous polymerized melts D^{Hf}/D^{Zr} for zircon is 0.5 to 0.2. Consequently, zircon fractionation will strongly decrease Zr/Hf in some granites. As Mn is geochemically similar to Fe, the planetary Fe/Mn ratio is approximately constant, corresponding to ~ 54 – 58 in various MORB basalts (Qin and Humayun 2008). Thus the Fe/Mn ratio near 50 dominates in majority of crustal rocks.

In addition to these data, strong evidence in favour of a garnetiferous leucogranitic protolith for felsic gneisses is provided by large, relict almandine- and spessartine-rich garnet porphyroclasts (2 to 3 cm in diameter) with P_2O_5 contents in the range of 0.1 to 0.5 wt. % (Tab. 7, Figs 6a–b). Garnet porphyroclasts contain approx. 50 vol. % of intergrown quartz, which escaped mylonitic deformation. The garnet–quartz intergrowth pattern is analogous to that observed in some unmetamorphosed Variscan garnetiferous leucogranites (Fig. 7) (Breiter et al. 2003; Vrána 2005; René and Stelling 2007). As indicated by comparison of the whole-rock analyses 1 and 2, an average for five whole-rock analyses published by Fiala (1992), and our results of microscopic and microprobe study, the felsic gneisses are characterised by minimal variation in composition.

During a superimposed event of pervasive shearing, mylonitization, fabric flattening and moderate-temperature, but high-pressure (MT/HP) re-equilibration (D_3 , M_3), the leucogranitic bodies were structurally transposed (refoliated) together with the surrounding rocks of the Malín Unit. Primary quartz mosaic was transposed to quartz ribbons or elongated lenticular aggregates. Variation in the Ky/Ms ratio in laminae across the foliation can be interpreted as resulting from variable hydrous fluid activity, since any indications of replacement relations between Ms and Ky are absent. Although kyanite–garnet–muscovite felsic gneisses from Bohouňovice and Suchdol were sometimes designated as “leptynite” (Fiala et al. 1982; Fiala 1992), or considered to be rocks with some relation to granulites, it is obvious that such relationship is based only on a macroscopic resemblance, whereby abundant small garnets are set in a fine-grained felsic matrix. However, the metamorphic record of the gneisses corresponds solely to amphibolite-facies conditions.

7.2. Possible ultrahigh-pressure history of leucosome from migmatite, indicated by the high sodium content in garnet

Large syn-migmatization garnets (1 to 4 mm in diameter) contain 0.05 to 0.10 wt. % Na_2O , accompanied by somewhat elevated phosphorus (Tab. 4). Such high sodium values are indicative of ultrahigh-pressure (UHP) conditions, as described from Dabie Shan and Dabie Sulu UHP terranes in China (Enami et al. 1995; Carswell et al. 2000) and for diamond-bearing detrital assemblages in the Bingara Area, Eastern Australia (Barron et al. 2005). According to Barron et al. (2005), high-sodium, Alm–Sps-rich garnets are interpreted as being derived from deeply subducted tonalitic and granitic gneisses, although some samples with increased Prp and Grs components also occur. The low grossular content reflects a low-Ca nature of the granitic gneisses. There is some uncertainty concerning the meaning of the calculated pressure value of 1.6 GPa for sample 4, which is definitely far beyond the UHP realm. Admittedly, there is a problem concerning the equilibrium between the large garnet grains and the matrix albite. Given the limited compositional data, it is preferable to consider the increased sodium contents in sample 4 as a probable or potential indication of a UHP event in the history of the sample, which could be confirmed only by a detailed study.

7.3. Crystallization of borosilicates

As tourmaline and dumortierite in samples 3 and 4 occur in different parts of thin sections, the mutual temporal relations of these minerals are difficult to assess.

However, both minerals are post- D_3 and may be closely related in time.

Regional information shows that tourmaline has been often observed in the muscovite–biotite gneisses and schists in the Malín Unit. As these rocks, in part migmatitic, predominate in the area, it is probable that alteration of tourmaline during M_3 supplied boron needed for crystallization of minor late borosilicates in the studied felsic gneisses. In general, in the KHC and the Svatka Unit, tourmaline is present in paragneisses with tourmalinite layers (Čopjaková et al. this volume), in some quartz–feldspar leucosomes and in hydrothermal quartz–tourmaline veinlets. There is no evidence for the presence of primary magmatic tourmaline in the protolith of the felsic gneisses (samples 1 to 3). However, primary tourmaline, if present formerly in the rock, would represent an alternative source for the late dravite–schorl and dumortierite growth.

The high-grade felsic kyanite–garnet granulites in the Běstvína Unit are completely free of borosilicates. One occurrence of dumortierite-bearing pegmatite in the Běstvína granulites, emplaced after culmination of the granulite HP/HT conditions, has been described by Cempírek and Novák (2006). The regional coincidence in occurrences of dumortierite pegmatites (Fiala 1954; Lohert 1956a; Cempírek and Novák 2006), with numerous localities of accessory dumortierite in polymetamorphic gneisses and migmatites of the Malín Unit (Fig. 2), may indicate that dumortierite pegmatites were emplaced at a late stage related to the M_3 event. This is a preliminary suggestion requiring additional evidence.

7.4. Correlation of the Kutná Hora–Svatka Superunit with the Orlice–Sněžník (Orlice–Kłodzko) Unit (OSU) at the Czech–Polish border

Several aspects indicate that the Kutná Hora–Svatka Superunit (Fig. 1) can probably be correlated with the Orlice–Sněžník Unit (OSU) further northeast, at the Czech–Polish border (Verner et al. this volume). Important points for this correlation of the Kutná Hora–Svatka Superunit with the OSU are the following: a) dating of garnet clinopyroxenites and associated pyrope lherzolite from Bečváry at approximately 377 ± 20 Ma (Brueckner et al. 1991) and indication of prolonged annealing of pyrope lherzolites in KHC following from study of mineral inclusions in pyrope (Vrána 2008); b) geochemical correlation of (Cambro–Ordovician) Svatka metagranite/orthogneiss with orthogneisses in the Orlické hory Mts. indicates a close similarity (Buriánek et al. this volume); c) comparison of the whole-rock geochemistry of mica schists and migmatites of the Svatka Unit with paragneisses and migmatites of the adjacent part of the

Moldanubian Zone (Strážek Unit) shows that the former were derived from geochemically more evolved and differentiated source (unpublished data). The main obstacle to closer correlation is the paucity of geochronological data on KHC rocks.

7.5. Correlation of the Kutná Hora–Svatka Superunit with the Moldanubian Zone in terms of metamorphism

The main difference between the Moldanubian Zone and KHC is in that in latter unit decompression proceeded dominantly in the kyanite field whereas, in the Moldanubian rocks, decompression was one of a prominent, nearly isothermal uplift with widespread neof ormation of sillimanite, replacement of kyanite by hercynitic spinel and/or low-Ca garnet, and crystallization of cordierite (Owen and Dostal 1996; Tajčmanová et al. 2006). These relations suggest that the KHC and the Moldanubian complex evolved separately for much of their Variscan tectonometamorphic history. The repetitive high-pressure record manifested in the KHC by M_1 (eclogite-facies granulites, $P \sim 2.0$ GPa), M_2 migmatites with Ky-bearing leucosome (eclogite-facies, 1.6 GPa), M_3 recrystallization related to penetrative shearing (HP amphibolite-facies, 1.1 GPa) represents a unique record at the present stage of knowledge of the Bohemian Massif. Clarification of the time and space relations between M_1 and M_2 requires additional data, as it is concerned with the allochthonous position of HP/HT Běstvína Unit granulites in the KHC. It is probable that the M_1 and M_2 events corresponded to Palaeo-Variscan processes (older than 340 Ma) and the M_3 event to Neo-Variscan processes (~ 340 Ma, coeval with the exhumation of the Moldanubian Zone).

8. Conclusions

In the Kutná Hora Complex, there are several types of albite–K-feldspar kyanite–garnet felsic gneisses, polymetamorphic migmatites and granulites. The felsic gneisses from Bohouňovice and Suchdol (Malín Unit, samples 1 and 2) formed by a late penetrative shearing and M_3 metamorphism of a primary, highly evolved, garnetiferous leucogranite. The protolith for sample 3 from Vysoká (Malín Unit) remains uncertain, though it was also a highly fractionated albitic rock. A leucosome from a polymetamorphic migmatite (sample 4, Malín Unit) exhibits effects of D_3 deformation and partial modification by superimposed M_3 metamorphism, but its garnet and coarse kyanite are interpreted as having been formed during the M_2 high-pressure migmatization event. Felsic HP/HT albite–K-feldspar granulites from the Běstvína Unit, samples 5 and 6, exhibit only the

near-peak metamorphic mineral assemblage. Geochemical data suggest a highly evolved magmatic protolith for this rock, but essentially different from that for felsic gneisses in the Malín Unit.

The published scheme of deformation events (D_1 to D_3) and polymetamorphism (M_1 to M_3) proved to be applicable for description of the record registered in the studied sample set. This scheme of events is very different from the record observed in the regionally neighbouring rocks of the Moldanubian Zone. The main difference is in that in KHC decompression proceeded dominantly in the kyanite field whereas, in the Moldanubian rocks, decompression was one of a prominent, nearly isothermal uplift with widespread neof ormation of sillimanite, replacement of kyanite by hercynitic spinel and/or low-Ca garnet, and crystallization of cordierite.

Textural and compositional data of metamorphic dravite–schorl tourmaline and dumortierite in the felsic gneisses may be used for interpretation of the probable emplacement time of dumortierite pegmatites described from the Kutná Hora region in the literature.

Acknowledgements We studied the felsic gneisses within the framework of the project: “Investigation of lithologically contrasting rocks in the crystalline units at the NE margin of the Moldanubian Zone” headed by J. Pertoldová. We would like to thank P. Škoda, Faculty of Science, Brno, for microprobe analyses, K. Kullerud and R. Kryza for critical comments and constructive reviews of the manuscript. Microprobe analyses of minerals were recalculated to the numbers of atoms using worksheets presented by A. Tindle at <http://www.open.ac.uk/earth-research/tindle/AGTWebPages/AGTSoft.html>. Data handling, recalculation and plotting were performed using the R language package *GCDkit* (Janoušek et al. 2006b).

Electronic supplementary material. The GPS coordinates of the studied samples, and the tables of whole-rock geochemical data (Tabs 2–3) are available online at the Journal web site (<http://dx.doi.org/10.3190/jgeosci.045>).

References

- ALCOCK J (1996) Effect of grossular on garnet-biotite, Fe-Mg exchange reactions: evidence from garnet with mixed growth and diffusion zoning. *Contrib Mineral Petrol* 124: 209–215
- BARRON BJ, BARRON LM, DUNCAN G (2005) Eclogitic and ultrahigh-pressure crustal garnets and their relationship to Phanerozoic subduction diamonds, Bingara Area, New England Fold Belt, Eastern Australia. *Econ Geol* 100: 1565–1582
- BOYNTON WV (1984) Cosmochemistry of the rare earth elements: meteorite studies. In: HENDERSON P (ed) *Rare Earth Element Geochemistry*. Elsevier, Amsterdam, pp 63–114
- BREITER K, SCHARBERT S (1998) Latest intrusions of the Eisgarn Pluton (South Bohemia–Northern Waldviertel). *Jb Geol B–A* 141: 25–37
- BREITER K, BERAN A, BURIÁNEK D, CEMPÍREK J, DUTROW B, HENRY D, NOVÁK M, POVONDRA P, RAIMBAULT L (2003) Příbyslavice near Čáslav, locality No. 10. In: NOVÁK M (ed) *Field Trip Guidebook, International Symposium on Light Elements in Rock-forming Minerals*. Masaryk University, Brno, pp 77–90
- BRUECKNER HK, MEDARIS LG, BAKUN-CZUBAROW N (1991) Nd and Sr age and isotope patterns from Variscan eclogites of the eastern Bohemian Massif. *Neu Jb Mineral, Abh* 163: 169–196
- BURIÁNEK D, VERNER K, HANŽL P, KRUMLOVÁ H (2009) Ordovician metagranites and migmatites of the Svratka and Orlice–Sněžník Units, northeastern Bohemian Massif. *J Geosci* 54: 181–200
- CARSWELL DA, WILSON RN, ZHAI M (2000) Metamorphic evolution, mineral chemistry and thermobarometry of schists and orthogneisses hosting ultra-high pressure eclogites in the Dabieshan of Central China. *Lithos* 52: 121–155
- CEMPÍREK J, NOVÁK M (2006) Mineralogy of dumortierite-bearing pegmatites at Starkoč and Běstvína, Kutná Hora Crystalline Complex. *J Czech Geol Soc* 51: 259–270
- ČERNÝ P, ERCIT TS (2005) The classification of granitic pegmatites revisited. *Canad Mineral* 43: 1601–1622
- ČOPIJKOVÁ R, BURIÁNEK D, ŠKODA R, HOUZAR S (2009) Tourmalinites in the metamorphic complex of the Svratka Unit (Bohemian Massif): a study of compositional growth of tourmaline and genetic relations. *J Geosci* 54: 221–243
- DOSTAL J, CHATTERJEE AK (2000) Contrasting behaviour of Nb/Ta and Zr/Hf ratios in a peraluminous granitic pluton (Nova Scotia, Canada). *Chem Geol* 163: 207–218
- ENAMI M, CONG B, YOSHIDA T, KAWABE I (1995) A mechanism for Na incorporation in garnet: An example from garnet in orthogneiss from the Dabie Sulu terrane, eastern China. *Amer Miner* 40: 475–482
- FARYAD SW (2009) The Kutná Hora Complex (Moldanubian zone, Bohemian Massif): a composite of crustal and mantle rocks subducted to HP/UHP conditions. *Lithos* 109: 193–208
- FERRY JM, SPEAR FS (1978) Experimental calibration of the partitioning of Fe and Mg between biotite and garnet. *Contrib Mineral Petrol* 66: 113–117
- FIALA F (1954) Dumortierite from Miskovice. *Sbor Nár Mus Prague* 10B, 2: 3–38 (In Czech)
- FIALA J (1992) Bořetice, granulitic layer in paragneiss of Malín Formation, Stop 17. In: FIALA J, FIŠERA M,

- JELÍNEK E, SLABÝ J, VRÁNA S (eds) High-Pressure Granulites – Lower Crustal Metamorphism, Excursion guide. Czech Geological Survey, Prague, pp 50–52
- FIALA J, LANG M, OBRDA J, PIVEC E, ULRYCH J (1982) Petrology of some garnet–kyanite–K-feldspar leptynites of the Czech Moldanubicum (Czechoslovakia). *Rozpr Čs Akad Věd, ř Mat Přír Věd* 92: 1–85
- FIALA J, MATĚJOVSKÁ O, VAŇKOVÁ V (1987) Moldanubian granulites and related rocks: petrology, geochemistry and radioactivity. *Rozpr Čs Akad věd, ř Mat Přír Věd* 97: 1–102
- FIŠERA M (1977) Geology and petrology of the Kutná Hora Unit west of Kolín. *Czech Geological Survey Research Papers* 16: 19–31 (in Czech)
- GREEN DH, LAMBERT IB (1965) Experimental crystallisation of anhydrous granite at high pressures and temperatures. *J Geophys Res* 70: 5259–5268
- GREW ES (1996) Borosilicates and boron in rock-forming minerals in metamorphic environments. In: GREW ES, ANOVITZ LM (eds) *Boron, Mineralogy, Petrology and Geochemistry*. Mineralogical Society of America Reviews in Mineralogy 33: 387–502
- INDARES A, MARTIGNOLE J (1985) Biotite–garnet geothermometry in the granulite facies: the influence of Ti and Al in biotite. *Amer Miner* 70: 272–278
- JANOUŠEK V, FINGER F, ROBERTS MP, FRÝDA J, PIN C, DOLEJŠ D (2004) Deciphering petrogenesis of deeply buried granites: whole-rock geochemical constraints on the origin of largely undepleted felsic granulites from the Moldanubian Zone of the Bohemian Massif. *Trans Roy Soc Edinb, Earth Sci* 95: 141–159
- JANOUŠEK V, GERDES A, VRÁNA S, FINGER F, ERBAN V, FRIEDL G, BRAITHWAITE CJR (2006a) Low-pressure granulites of the Lišov Massif, southern Bohemia: Viséan metamorphism of Late Devonian plutonic arc rocks. *J Petrol* 47: 705–744
- JANOUŠEK V, FARROW CM, ERBAN V (2006b) Interpretation of whole-rock geochemical data in igneous geochemistry: introducing Geochemical Data Toolkit (*GCDkit*). *J Petrol* 47: 1255–1259
- JANOUŠEK V, KRENN E, FINGER F, MÍKOVÁ J, FRÝDA J (2007) Hyperpotassic granulites from the Blanský les Massif (Moldanubian Zone, Bohemian Massif) revisited. *J Geosci* 52: 73–112
- KOTKOVÁ J (2007) High-pressure granulites of the Bohemian Massif: recent advances and open questions. *J Geosci* 52: 45–71
- KOZIOL AM, NEWTON RC (1988) Redetermination of the anorthite breakdown reaction and improvement of the plagioclase–garnet–Al₂SiO₅–quartz geobarometer. *Amer Miner* 76: 216–223
- KRETZ R (1983) Symbols for rock-forming minerals. *Amer Miner* 68: 277–279
- LE MAITRE RW (ed.) (1989) *A Classification of Igneous Rocks and Glossary of Terms*. Blackwell Scientific Publications, Oxford, pp 1–193
- LINNEN RL, KEPPLER H (2002) Melt composition control of Zr/Hf fractionation in magmatic processes. *Geochim Cosmochim Acta* 66: 3293–3301
- LOSERT J (1956a) Dumortierites from the migmatites and pegmatites in the vicinity of Kutná Hora. *Rozpr Čs Akad Věd, ř Mat Přír Věd* 66: 1–44 (in Czech)
- LOSERT J (1956b) Report on detailed geological mapping in the northern part of the Kutná Hora ore district. *Zpr geol výzk v Roce 1955*: 99–101 (in Czech)
- LOSERT J (1967) Contribution to the problem of the pre-Assyntian tectogenesis and metamorphism in the Moldanubicum of the Bohemian Massif. *Krystalinikum* 5: 61–84
- MEDARIS LG JR, GHENT ED, WANG HF, FURNELL JH, JELÍNEK E (2006) The Spačice eclogite: constraints on the P–T–t history of the Gföhl granulite terrane, Moldanubian Zone, Bohemian Massif. *Mineral Petrol* 86: 203–220
- NAHODILOVÁ R, FARYAD SW, PERTOLDOVÁ J, KONOPÁSEK J, ŠTĚDRÁ V (2005) HP melting and its relationship to the granulite facies metamorphism – an example of the “Gföhl nappe” in the Kutná Hora Crystalline Complex. *Geolines* 19: 86–87
- NAHODILOVÁ R, FARYAD S, PERTOLDOVÁ J, KONOPÁSEK J, ŠTĚDRÁ V (2006) The different metamorphic evolution of HP rocks of the Gföhl Unit in Kutná Hora Crystalline Complex against in Moldanubian Zone in Austria. *Geolines* 20: 98–99
- O'BRIEN PJ, RÖTZLER J (2003) High-pressure granulites: formation, recovery of peak conditions and implications for tectonics. *J Metamorph Geol* 21: 3–20
- OWEN JV, DOSTAL J (1996) Prograde metamorphism and decompression of the Gföhl gneiss, Czech Republic. *Lithos* 38: 259–270
- POWELL R, HOLLAND T, WORLEY B (1998) Calculating phase diagrams involving solid solutions via non-linear equations, with examples using THERMOCALC. *J Metamorph Geol* 16: 577–588
- QUIN L, HUMAYUN M (2008) The Fe/Mn ratio in MORB and OIB determined by ICP-MS. *Geochim Cosmochim Acta* 72: 1660–1677
- RECHE J, MARTINEZ FJ (1996) GPT: an Excel spreadsheet for thermobarometric calculations in metapelitic rocks. *Comput and Geosci* 22: 775–784
- RENÉ M, STELLING J (2007) Garnet-bearing granite from the Třebíč Pluton, Bohemian Massif (Czech Republic). *Mineral Petrol* 91: 55–69
- SELWAY JB, NOVÁK M (1997) Experimental conditions, normalization procedures and used nomenclature for tourmaline. NOVÁK M, SELWAY JB (eds) *Symposium Tourmaline 1997, Field Trip Guidebook*, Nové Město, pp 19–21
- SPEAR FS (1993) *Metamorphic Phase Equilibria and Pressure-Temperature-Time Paths*. Mineralogical Society of America Monograph, pp 1–799

- SYNEK J, OLIVERIOVÁ D (1993) Terrane character of the north-eastern margin of the Moldanubian Zone: the Kutná Hora Crystalline Complex, Bohemian Massif. *Geol Rundsch* 82: 566–582
- ŠTĚDRÁ V, ČÁP P, ČECH S, DOSBABA M, DUŠEK K, HOLÁSEK O, HRADECKÁ L, KADLECOVÁ R, MAŠEK D, ONDOVČIN T, REJCHRT M, SKÁCELOVÁ D, SKÁCELOVÁ Z, ŠVÁBENICKÁ L, VODRÁŽKA R (2009) Geological map 1 : 25 000 of the Czech Republic with explanations, sheet 13-324 Kutná Hora. Czech Geological Survey, Prague
- TAJČMANOVÁ L, KONOPÁSEK J, SCHULMANN K (2006) Thermal evolution of the orogenic lower crust during exhumation within a thickened Moldanubian root of the Variscan belt of Central Europe. *J Metamorph Geol* 24: 119–134
- VERNER K, BURIÁNEK D, VRÁNA S, VONDRŮVÍČEK L, PERTOLDOVÁ J, HANŽL P, NAHODILOVÁ R, P (2009) Tectonometamorphic features of geological units along the northern periphery of the Moldanubian Zone (Bohemian Massif). *J Geosci* 54: 87–100
- VRÁNA S (1989) Perpotassic granulites from southern Bohemia, a new rock type derived from partial melting of crustal rocks under upper mantle conditions. *Contrib Mineral Petrol* 103: 510–522
- VRÁNA S (2005) Almandine–spessartine garnet from Zajíčkov near Pelhřimov, Czech Republic. *Bull mineral-petrolog Odd Nár Muz (Praha)* 13: 232–233 (In Czech)
- VRÁNA S (2008) Mineral inclusions in pyrope from garnet peridotites, Kolín area, central Czech Republic. *J Geosci* 53: 17–30
- VRÁNA S, ŠTĚDRÁ V, FIŠERA M (2005) Petrology and geochemistry of the Běstvína granulite body metamorphosed at eclogite facies conditions, Bohemian Massif. *J Czech Geol Soc* 50: 95–106
- WILLIAMS ML, GRAMBLING JA (1990) Manganese, ferric iron, and the equilibrium between garnet and biotite. *Amer Miner* 75: 886–908